Esther Ochoa Fernández

CO_2 Acceptors for Sorption-Enhanced Steam Methane Reforming

Thesis for the degree of doktor ingeniør

Trondheim, June 2007

Norwegian University of
Science and Technology
Faculty of Natural Sciences and Technology
Department of Chemical Engineering

NTNU
Innovation and Creativity

NTNU
Norwegian University of Science and Technology

Thesis for the degree of doktor ingeniør

Faculty of Natural Sciences and Technology
Department of Chemical Engineering

ISBN 978-82-471-2842-8 (printed ver.)
ISBN 978-82-471-2856-5 (electronic ver.)
ISSN 1503-8181

Theses at NTNU, 2007:130

Printed by Tapir Uttrykk

Abstract

Sorption-enhanced steam methane reforming (SESMR) is an emerging technology for H_2 production from fossil fuels with CO_2 capture. The aim of the present work has been to study SESMR with a multiscale approach and to gain insight into certain aspects of the process.

Special attention has been given to the development of new high-temperature CO_2 acceptors and their impact on the workability of SESMR. The preparation and CO_2 capture properties of Li_2ZrO_3, potassium promoted Li_2ZrO_3, and Na_2ZrO_3 have been studied in detail. A novel soft-chemistry route has been developed with success for the synthesis of mixed oxides. This method involves intimate mixture of the precursors and requires lower temperatures than conventional solid-state routes, forming nanosized crystals with high purities. The properties of the powders such as capture rate of CO_2 and regeneration conditions have been significantly improved.

Nanocrystalline tetragonal Li_2ZrO_3 could hold CO_2 in amounts equivalent to 27 wt%, and saturation was reached in less than 5 min at 848 K and 100% of CO_2. These results represent important improvements in the carbon dioxide capture rates compared to monoclinic Li_2ZrO_3 prepared by solid-state reactions. However, low capture rates were observed when operating at CO_2 partial pressures lower than 0.2 bar. Controlling the Li:Zr ratio, and especially ensuring the presence of free ZrO_2, allowed improved uptake rates. More beneficial was the promotion of oxide with potassium due to the presence of molten carbonates. It is generally accepted that doping with potassium favours the diffusion of CO_2 through the Li_2CO_3 layer that is formed at the surface of the acceptor during the capture reaction. On the other hand, nanocrystalline monoclinic Na_2ZrO_3 showed superior uptake kinetics and the ability to work efficiently at CO_2 partial pressures as low as 0.025 bar. However, Na_2ZrO_3 required higher temperatures for regeneration.

The stability of the acceptors was studied both in dry and wet conditions. The powders showed good stability when treated in dry environments. However, although the presence of steam was beneficial for the capture and regeneration kinetics, steam had a negative impact on the stability and a continuous decay was observed for all samples. The decay was most pronounced for potassium promoted Li_2ZrO_3 and Na_2ZrO_3.

A fixed-bed reactor was used to test the ability of these materials in SESMR. A Ni-Mg-Al hydrotalcite-like catalyst with 40 wt% Ni and proven stability and activity for steam methane reforming (SMR) was used as a catalyst. Hydrogen concentrations above 97% on a dry basis were reached at 848 K, steam to carbon ratio 5, and 5 bar using Na_2ZrO_3 as acceptor. At such conditions the equilibrium concentration of H_2 in conventional SMR without CO_2 removal is 68%. However, no such enhancement in the H_2 yields was observed when using Li_2ZrO_3 as acceptor, due to kinetic limitations during the CO_2 removal. On the other hand, it was observed that the alkaline acceptors interact with the catalyst, resulting in catalyst deactivation.

A process design simulation of H_2 production by SESMR was also carried out. A concept for pure H_2 production with CO_2 capture by SESMR was proposed and compared to conventional SMR with CO_2 capture. It was concluded that the thermal efficiency of the process will depend strongly on the selected CO_2 acceptor. The thermal efficiencies of SESMR using the alkaline acceptors were comparable to conventional steam reforming, approximately 70-72%. The use of an acceptor with more favourable thermodynamics for CO_2 removal, such as CaO, considerably enhanced this efficiency to about 80%.

The results from this thesis suggest that SESMR can be a promising alternative for production of hydrogen and power generation with CO_2 management. SESMR results in a simpler process configuration, less demand for high temperature materials and reasonable thermal efficiency when compared to SMR. The alkaline acceptors studied here have shown excellent properties for CO_2 removal especially at dry conditions. However, further work is necessary in order to apply them to processes as SESMR, including improvement of the stability in wet atmospheres and integration with the reforming catalyst.

Acknowledgements

First of all, I would like to express my most sincere gratitude to my supervisor Professor De Chen for his support, guidance and encouragement throughout the work with this thesis. Your never-ending enthusiasm and ideas have been of great help. I would also like to acknowledge Associate Professor Magnus Rønning for his always positive attitude and valuable comments.

I am very grateful to have had the opportunity to cooperate with many different people during the last four years. Discussions about materials science with Professor Tor Grande have been very interesting and instructive. I would also like to thank Professor Hugo A. Jakobsen and Hans Kristian Rusten for great teamwork and introducing me, an experimentalist, into the world of reactor modelling. Thanks for your patience! Meetings with Inge Hovd Gangås at the Technology Transfer Office have also been very interesting and given me the opportunity to see science from a very different perspective. Tiejun Zhao, Claudia Lacalle-Vilà and Geir Haugen are also acknowledged for their contribution to this thesis and good collaboration.

When working in a lab and dealing with large setups, technical problems are difficult to avoid. Edvard Bergene, De Chen, Jan Morten Roel and Jan Erik Aastad are gratefully acknowledged for technical support and teaching me some of their tricks. Elin Nilsen is also thanked for her always kind assistance with X-ray diffraction.

The financial support from the Research Council of Norway through the KOSK programme and the Department of Chemical Engineering is greatly acknowledged.

I also want to thank all my colleagues at NTNU and SINTEF for their support, friendship and great working environment. I would especially like to mention my office mate Ingvar Kvande for all our relevant and less relevant discussions which have made the last four years very enjoyable.

During this period of time I have met many different people and made friends from all over the world. I am grateful for all the great moments we have had together. I, of course, have to mention the Settlers team. Thanks for keeping me busy during the last months thinking, at least temporarily, of something else than this thesis.

I very much want to thank my family for always supporting me and being the first ones to encourage me when I decided to start my Norwegian adventure. I would never have gone so far in life without you. Os quiero mucho! My best wishes also to my friends in Spain that have been supporting me from a distance making me feel like I never left. Muchas gracias a todos!

Finally, my special thanks go to Øyvind for his love, support, and all the special moments shared together since the first day. The last few months have been hard for us with two theses to defend, but we have been a very strong team! New times are about to come, and I am looking forward to sharing them with you!

List of publications and presentations

Publications

This thesis is based on the following papers enclosed as appendices.

I. E. Ochoa-Fernández, M. Rønning, T. Grande, and D. Chen. Nanocrystalline Lithium Zirconate with Improved Kinetics for High-Temperature CO_2 Capture. *Chem. Mater.*, 18:1383-1385, 2006.

II. E. Ochoa-Fernández, M. Rønning, T. Grande, and D. Chen. Synthesis and CO_2 Capture Properties of Nanocrystalline Lithium Zirconate. *Chem. Mater.*, 18:6037-6046, 2006.

III. E. Ochoa-Fernández, M. Rønning, X. Yu, T. Grande, and D. Chen. Compositional effects of nanocrystalline lithium zirconate on its CO_2 capture properties. Submitted to *Ind. Eng. Chem. Res.*

IV. T. Zhao, E. Ochoa-Fernández, M. Rønning, and D. Chen. Preparation and High-Temperature CO_2 Capture Properties of Nanocrystalline Na_2ZrO_3. *Chem. Mater.*, DOI:10.1021/cm062732h, 2007.

V. E. Ochoa-Fernández, M. Rønning, and D. Chen. Effects of steam addition on the properties of high temperature CO_2 ceramic acceptors. In preparation.

VI. E. Ochoa-Fernández, C. Lacalle-Vilà, K. O. Christensen, M. Rønning, A. Holmen, and D. Chen. Ni catalysts for sorption enhanced steam methane reforming. *Top. Catal.*, DOI: 10.1007/s11244-007-0231-x, 2007.

VII. E. Ochoa-Fernández, C. Lacalle-Vilà, T. Zhao, M. Rønning, and D. Chen. Experimental Demonstration of H_2 Production by CO_2 Sorption Enhanced Steam Methane Reforming Using Ceramic Acceptors. Accepted *Stud. Surf. Sci. Catal.*, 2007.

VIII. E. Ochoa-Fernández, G. Haugen, T. Zhao, M. Rønning, I. Aartun, B. Børresen, E. Rytter, M. Rønnekleiv, and D. Chen. Process design simulation of H_2 production by sorption enhanced steam methane reforming: evaluation of potential CO_2 acceptors. *Green Chem.*, DOI: 10.1039/b614-270b, 2007.

Additional publications and conference proceedings

A list of additional publications and conference proceedings where the author has also been involved during the PhD period is presented here.

- D. Chen, E. Ochoa-Fernández, M. Rønning, and T. Grande. Carbon dioxide acceptors. *PCT Int. Appl.*, WO2006111343, 2006.
- H. K. Rusten, E. Ochoa-Fernández, D. Chen, and H. A. Jakobsen. Numerical investigation of sorption enhanced steam methane reforming using Li_2ZrO_3 as CO_2 acceptor. In press *Ind. Eng. Chem. Res.*, 2007.
- E. Ochoa-Fernández, G. Haugen, H. K. Rusten, T. Zhao, M. Rønning, H. A. Jakobsen, I. Aartun, B. Børresen, E. Rytter, M. Rønnekleiv, and D. Chen. Evaluation of potential CO_2 acceptors for application in hydrogen production by sorption enhanced steam methane reforming. *Prepr. Pap.-Am. Chem. Soc., Div. Fuel Chem.*, 51:598-599, 2006.
- E. Ochoa-Fernández, G. Haugen, H. K. Rusten, T. Zhao, M. Rønning, H. A. Jakobsen, I. Aartun, B. Børresen, E. Rytter, M. Rønnekleiv, and D. Chen. Design, preparation and applications of CO_2 acceptors in power generation with CO_2 management. Proceedings of the GHGT-8: *8th International Conference on Greenhouse Gas Control Technologies*, 19-22 June 2006, Trondheim, Norway.
- H. K. Rusten, E. Ochoa-Fernández, D. Chen, H. Lindborg, and H. A. Jakobsen. Modeling and simulation of sorption enhanced hydrogen production. Proceedings of the GHGT-8: *8th International Conference on Greenhouse Gas Control Technologies*, 19-22 June 2006, Trondheim, Norway.

- E. Ochoa-Fernández, H. K. Rusten, H. A. Jakobsen, M. Rønning, A. Holmen, and D. Chen. Sorption enhanced hydrogen production by steam methane reforming using Li_2ZrO_3 as sorbent: sorption kinetics and reactor simulation. *Catal. Today*, 106:41-46, 2005.

Presentations

A list of oral and poster presentations is listed below. The presenter is typeset in bold face.

- E. Ochoa-Fernández, C. Lacalle-Vilà, T. Zhao, M. Rønning, and ***D. Chen***. H_2 production by CO_2 sorption enhanced steam methane reforming using ceramic acceptors. Oral presentation. 8th Natural Gas Conversion Symposium, 27-31 May 2007, Natal, Brazil.

- ***E. Ochoa-Fernández***, G. Haugen, T. Zhao, M. Rønning, I. Aartun, B. Børresen, E. Rytter, M. Rønnekleiv, and D. Chen. Evaluation of potential CO_2 acceptors for application in hydrogen production by sorption enhanced steam methane reforming. Oral presentation. 232th ACS National Meeting, 10-14 September 2006, San Francisco, USA.

- ***T. Zhao***, E. Ochoa-Fernández, M. Rønning, J. Zhu, W. Yuan, and D. Chen. Fabrication and high-temperature carbon dioxide capture properties of nanocrystalline sodium zirconate. Poster presentation. 19th International Symposia on Chemical Reaction Engineering, ISCRE-19, 3-6 September 2006, Berlin, Germany.

- ***H. K. Rusten***, E. Ochoa-Fernández, D. Chen, and H. A. Jakobsen. Modelling and simulation of sorption enhanced steam reforming, integration of catalyst and adsorbent. Oral presentation. 19th International Symposia on Chemical Reaction Engineering, ISCRE-19, 3-6 September 2006, Berlin, Germany.

- ***H. K. Rusten***, E. Ochoa-Fernández, D. Chen, and H. A. Jakobsen. Heterogeneous and pseudo-homogeneous reactor models with solution of the velocity-pressure coupling for simulation of sorption enhanced steam reforming. Oral presentation. 17th International Congress of Chemical and Process Engineering, CHISA-17, 27-31 August 2006, Prague, Czech Republic.

- ***H. K. Rusten***, E. Ochoa-Fernández, D. Chen, E. Hessen, and H. A. Jakobsen. Modelling and simulation of sorption enhanced hydrogen production. Oral presentation. 12th International Conference on Greenhouse Gas Control Technologies, GHGT-8, 19-22 June 2006, Trondheim, Norway.

- ***E. Ochoa-Fernández***, G. Haugen, T. Zhao, H. K. Rusten, J. P. Andreassen, M. Rønning, H. A. Jakobsen, I. Aartun, B. Børresen, E. Rytter, M. Rønnekleiv, and D. Chen. Design, preparation and applications of CO_2 acceptors in power generation with CO_2 management. Oral presentation. 12th International Conference on Greenhouse Gas Control Technologies, GHGT-8, 19-22 June 2006, Trondheim, Norway.

- ***E. Ochoa-Fernández***, C. Lacalle-Vilà, T. Zhao, K. O. Christensen, M. Rønning, A. Holmen, and D. Chen. Catalyst and CO_2 acceptor evaluation for application in sorption enhanced steam methane reforming. Oral presentation, 12th Nordic Symposium on Catalysis, 28-30 May 2006, Trondheim, Norway.

- ***E. Ochoa-Fernández***, T. Zhao, G. Haugen, M. Rønning, and D. Chen. CO_2 acceptors for H_2 production by sorption enhanced steam methane reforming. Oral presentation, Nordic Hydrogen Seminar, 6-8 February 2006, Oslo, Norway.

- ***E. Ochoa-Fernández***, H. K. Rusten, H. A. Jakobsen, and D. Chen. Solid high temperature CO_2 sorbents for the production of H_2 by sorption enhanced steam reforming. Oral presentation. Gas-Fuel 05, 14-16 November 2005, Brugge, Belgium.

- ***H. K. Rusten***, E. Ochoa-Fernández, D. Chen, E. Hessen, and H. A. Jakobsen. Modelling and simulation of sorption enhanced hydrogen production. Oral presentation. The Third Trondheim Conference on CO_2 Capture, Transport and Storage, 10-11 October 2005, Trondheim, Norway.

- E. Ochoa-Fernández, T. Zhao, G. Haugen, H. K. Rusten, M. Rønning, H. A. Jakobsen, and ***D. Chen***. Application of CO_2 sorption enhanced hydrogen production with CO_2 removing: precombustion in power generation. Oral presentation. The Third Trondheim Conference on CO_2 Capture, Transport and Storage, 10-11 October 2005, Trondheim, Norway.

- ***E. Ochoa-Fernández***, T. Grande, H. K. Rusten, H. A. Jakobsen, A. Holmen, M. Rønning, and D. Chen. Novel solid high temperature CO_2 absorbents for the production of H_2 by sorption enhanced steam reforming. Poster presentation, EuropaCat-VII, 28 August - 1 September 2005, Sofia, Bulgaria.

- ***E. Ochoa-Fernández***, T. Grande, M. Rønning, and D. Chen. Structure and high temperature CO_2-sorption properties of lithium zirconate. Oral presentation, Norwegian hydrogen seminar, 15-16 December 2004, Kvitfjell, Norway.

List of symbols and abbreviations

Greek symbols

Symbol	Description	Unit
β	Experimental line width	rad
θ	Angle	rad
λ	X-ray wavelength	m
ρ	Density	kg m^{-3}
σ	Metallic surface area	m^2
ν	Stoichiometry of the reaction	-
$\Delta\omega$	Experimental CO_2 uptake	wt%
$\Delta\omega_{max}$	Maximum experimental CO_2 uptake	wt%

Latin symbols

Symbol	Description	Unit
A	Atomic weight	g mol^{-1}
D	Dispersion	%
d	Particle diameter	m
f	Fraction exposed to the surface	-
K	Constant	-
$< L >$	Particle size	m
M_i	Molecular weight of gas i	g mol^{-1}

Latin symbols (continued)

Symbol	Description	Unit
Δm	Mass change	g
N_A	Avogadros's number	mol^{-1}
P	Pressure	atm
R	Ideal gas constant	atm L K^{-1} mol^{-1}
S	Surface area	m^2
T	Temperature	K
T_c	Carbonation temperature	K
T_r	Regeneration temperature	K
t_o	Initial time	s
t_s	Saturation time	s
V	Volume	m^3
V_e	Tapered element void volume	L
W	Catalyst weight	kg
x	Extent of reaction	-
X	Conversion	%

Abbreviations

ATR	Autothermal reforming
BET	Brunauer-Emmett-Teller
BJH	Barrett-Joyner-Halenda
FESEM	Field emission scanning electron microscopy
GHG	Greenhouse gases
HT	Hydrotalcite
HTlc	Hydrotalcite-like compound
HTXRD	High-temperature X-ray diffraction
IEA	International Energy Agency
IPCC	Intergovernmental Panel on Climate Change
PEM	Proton exchange membrane
POX	Partial oxidation
PSA	Pressure swing adsorber/adsorption
PSD	Position sensitive detector
SERP	Sorption-enhanced reaction process
SESMR	Sorption-enhanced steam methane reforming
SMR	Steam methane reforming
STEM	Scanning transmission electron microscopy
S/C	Steam to carbon ratio

Abbreviations (continued)

TEOM	Tapered element oscillating microbalance
TPR	Temperature programmed reduction
WGS	Water gas shift
XPS	X-ray photoelectron spectroscopy
XRD	X-ray diffraction

Contents

Chapter 1

Introduction

1.1 Global warming

The average temperature of the Earth's atmosphere and oceans has increased dramatically in recent decades and it is projected to continue. The Intergovernmental Panel on Climate Change (IPCC) has predicted that global temperatures are likely to increase by 1.1 to 4.5 K between 1990 and 2100 [1]. Moreover, the scientific community has agreed that the main reason for global warming is the observed increase in anthropogenic greenhouse gas concentrations.

1.1.1 The greenhouse effect

The Earth has a natural greenhouse effect due to small amounts of H_2O and CO_2 that are naturally present in the atmosphere. The Earth receives energy from the sun in the form of short-wavelength radiation. Part of this radiation is reflected back to the atmosphere as infrared radiation, which is partially absorbed by the so-called greenhouse gases (GHG). This process, known as the natural greenhouse effect, regulates the Earth's temperature and allows life as known today. The major natural greenhouse gases are water vapour, carbon dioxide, methane, and ozone. The concentrations of several greenhouse gases have increased considerably over time due to human activities, resulting in global warming and climate change.

1.1.2 Energy consumption and CO_2 emissions

According to the International Energy Agency (IEA), the global consumption of energy and the associated emissions of the GHG CO_2 have continued in an upward trend the last 30 years [2]. Fossil fuels are the dominant form of energy utilised in the world (86%), accounting for about 75% of the current anthropogenic CO_2 emissions [1]. Figure 1.1 shows the global CO_2 emissions from fossil fuels from 1830 to present [3].

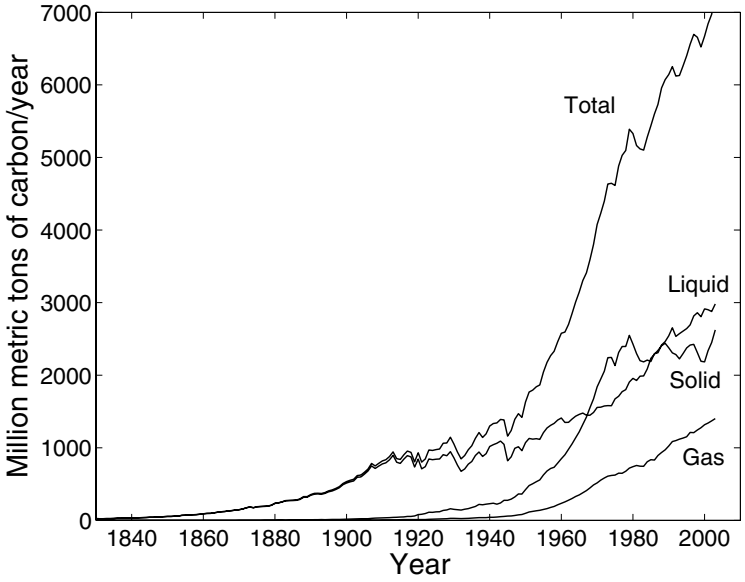

Figure 1.1: Global CO_2 emissions from fossil fuels [3].

The CO_2 emissions from various sectors have been estimated by IEA and power generation remains the single largest source of CO_2 emissions, emitting as much CO_2 as the rest of the industrial sector together, while the transport sector is the fastest-growing source of CO_2 emissions [2].

1.1.3 Strategies for mitigation of climate change

There exist different initiatives to mitigate the increase of carbon dioxide emissions [4]. Reductions in fossil fuel consumption can be achieved by improving the efficiency of energy conversion, for example by the use of improved turbines. Another way to minimise emissions is to switch to less carbon-intensive fossil fuels as natural gas and/or increase the use of low- and near-zero-carbon

energies, such as renewable energy or nuclear power. These measures can reduce CO_2 generation; however, in order to reach the specific atmospheric CO_2 levels set in different international agreements, the capture of CO_2 and its storage plays a very important role. An alternative is the sequestration of CO_2 through the enhancement of natural sinks, as forests and soils. However, the development of technology for capturing CO_2 generated by fuel combustion or released from industrial processes is crucial.

1.1.4 CO_2 capture technologies

The purpose of CO_2 capture is to produce a concentrated stream of CO_2 at high pressure that can be easily transported to a storage site. Depending on the process, there are three main approaches to capture the generated CO_2 [5]:

- ***Post-combustion systems*** separate the CO_2 from flue gases produced by the combustion of primary fossil fuels. Chemical absorption is the most important post-combustion CO_2 capture technology today. The absorption processes offer high capture efficiency and selectivity, and lower costs than other existing post-combustion processes. Emerging technologies include CO_2 adsorption processes, gas separation membranes and high temperature solid CO_2 acceptors.
- ***Pre-combustion systems*** separate the CO_2 before the combustion. This comprises a first stage where the primary fuel is generally converted into a mixture of hydrogen and carbon monoxide, typically by reforming or partial oxidation. Then, carbon monoxide is further transformed to CO_2 by the water-gas shift (WGS) reaction. The main advantage of pre-combustion systems is that they produce a fuel (hydrogen) that is essentially carbon-free. Emerging pre-combustion technologies include sorption enhanced reaction processes, membrane reactors with CO_2 capture and chemical looping.
- ***Oxy-fuel combustion systems*** use oxygen for combustion of the primary fuel, producing a flue gas that consists mainly of steam and CO_2, avoiding the dilution with nitrogen. One of the main challenges in oxy-fuel combustion is the high temperatures involved that make recirculation of flue gases through the combustion chamber necessary. Generation of large amounts of high purity oxygen also has to be considered.

Figure 1.2 shows an overview of the different CO_2 capture systems.

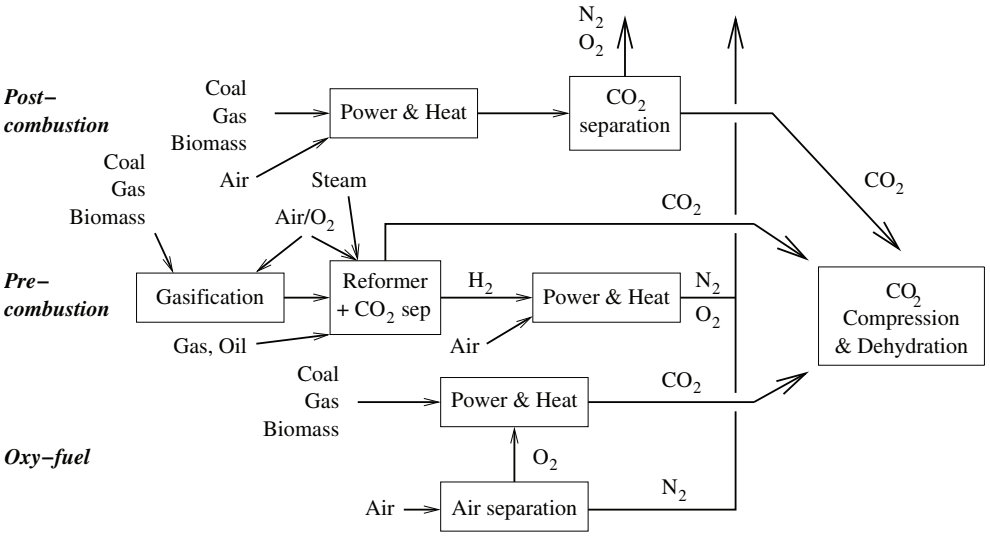

Figure 1.2: Technologies for CO_2 capture (from Bolland [5]).

1.1.5 CO_2 transport and storage

CO_2 is compressed before it is transported to possible storage sites. Compressed CO_2 (10 to 80 MPa) occupies around 0.2% of the volume of the gas at standard conditions. Transport is typically carried out by pipeline, by ship and by road tanker [4].

There exist several options for the storage of CO_2. The first alternative is injection of CO_2 into natural reservoirs, such as geological formations. CO_2 would be injected in the same way as CO_2 has been injected for enhanced oil recovery. Other alternatives include: using CO_2 to make chemicals, fixing it in mineral carbonates, storing it as solid CO_2 (dry ice), as CO_2 hydrates, or solid carbon.

1.2 The hydrogen economy

The idea of using hydrogen as a fuel is relatively old and dates from its isolation by Henry Cavendish in 1766, to the beginning of fuel-cell developments by W. R. Grove in 1839, to current times [6]. In fact, the depletion of fossil fuel resources and the increase in energy demand require development of alternative low-emission and low-carbon energy systems. In this sense, hydrogen is expected to play an important role as a future energy carrier.

1.2.1 Driving forces to a hydrogen economy

The largely fossil-fuel based economy is currently undergoing rapid changes because of the need of minimising air pollution. In addition, with the current level of global oil production, oil reserves will be sufficient for no more than 40 years [7]. Therefore, there exist several driving forces from a carbon-based towards a hydrogen-based society:

- ***Environmental protection:*** Hydrogen can be burned in an internal combustion engine, gas turbines or used in fuel cells to produce electricity and power, with water being the main by-product.
- ***Security of supply:*** The world energy demand is anticipated to grow significantly while the petroleum reserves are set to fall. Hydrogen is the most abundant element on Earth, and in addition, it has the most energy per unit mass (120 MJ/kg). Hydrogen can be stored in different forms and can serve as a storage for renewable energy to make it continuously available.
- ***Technological improvement:*** The future of the hydrogen society is strongly dependent on technological breakthroughs, both in technologies for hydrogen production (fossil fuels, renewable energies, electrolysis, biomass), storage and distribution, and end-use technology. The main challenges include the reduction of hydrogen production costs from different routes, research and development of CO_2 sequestration, improvement of hydrogen storage capacity, establishing distribution infrastructures, and the development of hydrogen gas turbines and fuel cell applications. All having the potential of reducing the total cost and of making the technology competitive.
- ***Social and economic development:*** The development of more efficient and cleaner energy systems will be directly translated into long-term social and economic benefits.

1.2.2 Hydrogen production

Hydrogen can be manufactured from a range of energy sources such as fossil fuels, biofuels, renewable sources and nuclear energy via electricity. Hydrogen can also readily be produced from synthesised hydrogen carriers such as methanol or ammonia [8]. Ideally, successful entry of the hydrogen economy

means economically viable hydrogen production using only renewable energy supplies. However, the most economical route for hydrogen production today is steam reforming of a hydrocarbon feedstock. In fact, natural gas is the preferred source of H_2 and syngas [9]. There are several methods for producing H_2 from natural gas including:

- ***Steam methane reforming (SMR):*** SMR uses an endothermic, catalysed reaction between natural gas and steam. Typical reaction conditions are 1073-1173 K and 20-40 bar. Heat is supplied to the reactor tubes by burning part of the fuel. The reformer gas is cooled and passed into the CO shift system before the H_2/CO_2 separation step. CO_2 can be removed by chemical absorption (amines, bicarbonates) or using a pressure swing adsorber (PSA). CO_2 separation results in a large penalty in the SMR efficiency.

- ***Partial oxidation (POX):*** In the POX process, a fuel reacts with pure oxygen at temperatures typically above 1273 K. The process is slightly exothermic and all the heat required for the reaction is supplied by partial combustion of the fuel, no external heat is required. As with SMR, the syngas will be cooled, shifted and the CO_2 removed from the mixture.

- ***Autothermal reforming (ATR):*** ATR can be considered as a combination of the two processes described above. ATR uses a partial oxidation burner followed by a catalyst bed with a feed of natural gas, steam and oxygen. The addition of steam enables a high conversion of fuel at a lower temperature than POX. CO_2 capture is carried out as described above for the SMR.

Emerging options in natural gas reforming incorporate novel combined reaction/separation systems such as sorption-enhanced steam methane reforming (SESMR) and membrane reforming.

H_2 inorganic membranes and CO_2 dense membranes offer the possibility of combining reaction and separation in a single step at high temperature and pressure, overcoming the equilibrium limitations of conventional configurations. As a result, a high-purity H_2 stream is obtained at the permeate side, leaving behind a retentate gas which is predominantly CO_2 and small amounts of unrecovered H_2 and steam [4]. The major challenge today is to develop membranes with good selectivity, stability and permeability [10].

SESMR uses a bed containing a mixture of a reforming catalyst and a selective acceptor to remove CO_2 at high temperatures from the reaction zone, shifting the equilibrium limitation of SMR [11]. The acceptor is then regenerated by a pressure or temperature swing process. Different acceptors have been identified in literature (e.g. CaO, hydrotalcites). The main problem associated with these materials is their inherent low capacity and/or the rapid decay in capacity during multi-cycle operation. Therefore, the development of novel CO_2 acceptors is essential for the future of SESMR.

1.3 Scope of the work

SESMR is an emerging technology for H_2 production from fossil fuels with CO_2 capture. The aim of the present work has been to study SESMR by a multiscale approach and gain insight into certain aspects of the process such as the role of the CO_2 acceptor, catalyst and efficiency.

Special attention has been given to the development of new high-temperature CO_2 acceptors. Alkaline zirconates have recently been reported as good candidates [12]. The high capture capacity and stability at relatively high temperatures of these ceramic materials make them very promising for application in both pre- and post-combustion systems. However, kinetic limitations during the CO_2 capture are still the main obstacle. These CO_2 acceptors have been conventionally prepared by solid-state reactions at high temperatures, using zirconium oxide and alkali salts as precursors. The resulting oxides often contain relatively large particles of low purity, leading to limited capacity and kinetics for CO_2 capture. One of the main objectives of this work has been to develop alternative synthesis routes for such materials, including Li_2ZrO_3 and Na_2ZrO_3, and study in detail their CO_2 capture and regeneration properties in dry and wet atmospheres, aiming at a better understanding of the relationship between the crystal structure of the materials and their properties as CO_2 acceptors.

Simultaneously, an effort has been done to prepare Ni catalysts with high activity and stability under normal operating conditions. SESMR is carried out at lower temperatures than conventional SMR, typically between 673 and 873 K and therefore, a very active reforming catalyst is necessary.

Experimental demonstration of H_2 production by SESMR using the in-house prepared materials in a fixed-bed reactor has been a further objective of this thesis.

Finally, process design has been used as a tool to optimise the system configuration, aiming to improve the heat integration and total efficiency of the system.

1.4 Thesis outline

This thesis is divided into five individual chapters. *Chapter 1* is an introduction to the background and motivations of this study.

In *Chapter 2*, a comprehensive review of the most relevant literature and theory related to high temperature CO_2 solid acceptors and SESMR is presented.

Chapter 3 describes the experimental techniques and procedures followed in the work, while *Chapter 4* summarises the main results and discussion.

Conclusions and recommendations for further work are included in *Chapter 5*.

The thesis is based on a collection of eight publications that are provided as appendices.

Paper I is a short communication describing the synthesis and CO_2 capture properties of nanocrystalline Li_2ZrO_3. A more complete investigation is included in *Paper II*.

Paper III deals with the study of the effect of different lithium zirconate stoichiometries on the working properties of the material. The effect of promoting Li_2ZrO_3 with potassium is also addressed.

Na_2ZrO_3 has also been proposed as a good candidate for CO_2 capture. The preparation, characterisation and properties of Na_2ZrO_3 as a CO_2 acceptor are the main objectives of *Paper IV*.

SESMR is carried out at large partial pressures of steam. Therefore, it is necessary to understand the effect of steam on the behaviour of the studied materials. This issue is addressed in *Paper V*.

Paper VI deals with an investigation on different Ni catalyst with high activity and stability for the application in SESMR.

The in-house prepared Ni catalyst and the CO_2 acceptors described in the above publications have been used to probe the feasibility of SESMR. This study is included in *Paper VII*.

Finally, process design simulation of H_2 production by sorption-enhanced steam methane reforming has been carried out. A concept for pure H_2 production with CO_2 capture by SESMR has been proposed and compared to conventional steam reforming with CO_2 capture (*Paper VIII*).

1.5 Author's contribution

The author has had an active role in all the stages of the work reported in this thesis. The author has planned, conducted and interpreted the results of most of the work reported here. However, some people have contributed to different parts of the work:

- Part of the experimental work in *Papers VI* and *VII* was performed by diploma student Claudia Lacalle-Vilà under supervision of the author.
- The electron microscopy images in *Paper VI* were taken by John C. Walmsley.
- Xiaofeng Yu conducted the X-ray photoelectron spectroscopy measurements in *Paper III*. The author interpreted the data with help from Steinar Raaen.
- Geir Haugen developed the Hysys model described in *Paper VIII* and helped interpreting the results of that section. This work was performed in collaboration with staff from Statoil Research Centre who contributed to the definition of the concept design.
- Tiejun Zhao planned and conducted most of the experiments in *Paper IV* with the assistance of the author.

The author wrote all the papers presented here with exception of *Paper IV*, however, she did play an active role in the writing.

Chapter 2

Theory and literature

2.1 Steam methane reforming

2.1.1 Reaction and thermodynamics

The principal process for converting methane into hydrogen is steam reforming, which involves the following reactions:

$$CH_4 + H_2O \Longleftrightarrow CO + 3H_2 \quad \Delta H^0_{298} = 206 \text{ kJ/mol} \tag{2.1}$$

$$CO + H_2O \Longleftrightarrow CO_2 + H_2 \quad \Delta H^0_{298} = -41 \text{ kJ/mol} \tag{2.2}$$

Reaction 2.1 represents the steam reforming of methane. It is reversible and strongly endothermic. In addition, the reaction is favoured at high temperatures, high steam-to-carbon ratio (S/C), and low pressures [13]. The produced carbon monoxide can further react with steam to produce more hydrogen via the water-gas shift reaction (reaction 2.2).

Figure 2.1 shows the equilibrium gas composition out of the steam reformer as a function of the outlet temperature under typical industrial conditions. Dry H_2 yields close to 75% can be obtained at operating temperatures above 1100 K, corresponding to a conversion of methane close to 85%.

2.1.2 New challenges for SMR due to the emerging H_2 economy

Traditionally, SMR has been carried out in side-fired tubular steam reformers. In recent years, there has been significant progress in medium to large scale

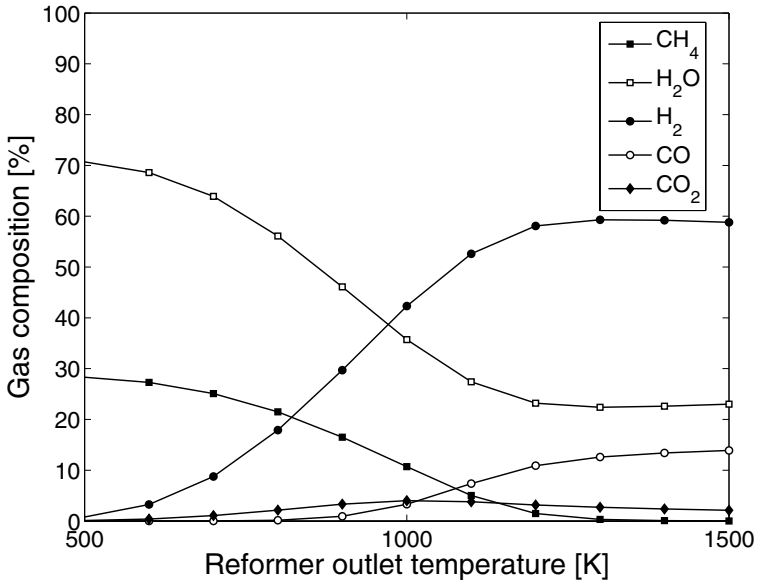

Figure 2.1: Equilibrium composition out of a steam methane reformer at 20 bar with a feed steam-to-carbon ratio of 2.5 (calculated from FactSage [14]).

hydrogen manufacture by steam reforming, mainly related to improved energy efficiency, reduced steam reformer size and cost [8]. Thus, it is reasonable to say that SMR is a mature technology that allows efficient production of H_2. However, the emerging hydrogen economy presents a new set of challenges to the SMR process [8].

Hydrogen can be produced with today's technology in large centralised plants at reasonable cost. The present use of manufactured H_2 is primarily for the production of ammonia and methanol, and for hydrotreatment in refineries. The emerging H_2 society, with for instance a hydrogen fuelled automotive sector, will increase the number of end users and distribution of H_2 will be an issue to consider. In fact, there is a high cost associated to H_2 distribution and safety issues are also of great concern. Therefore, increased interest is observed for smaller scale localised H_2 production, which requires the development of new reforming concepts.

On the other hand, the advantages of the H_2 society are unlikely to be realised until H_2 production with CO_2 sequestration becomes a reality. Finding a solution for delivering H_2 economically with sequestration of CO_2 is challenging.

One alternative that has been proposed is sorption-enhanced steam methane reforming, where reforming and CO_2 separation are carried out simultaneously in the reformer in the presence of CO_2 acceptors.

2.2 Sorption-enhanced steam methane reforming

2.2.1 Principle, reactions and thermodynamics

Conventional steam methane reforming involves multiple steps and severe operating conditions. The reformer is normally operated at 1073-1123 K, 20-30 bar and steam-to-carbon ratios between 2-4. The reactor effluent gas typically contains 70-72% H_2, 8-10 % CO, 10-14% CO_2 and 6-8% CH_4 on dry basis [15]. For further purification of the H_2, the reformer is followed by high and low temperature shift reactors, and occasionally a carbon dioxide removal step.

Hydrogen production by SESMR is an alternative to conventional SMR and combines reaction and separation in a single step. A CO_2 acceptor is installed together with the reforming catalyst in the reactor bed. In this way, the equilibrium of reactions 2.1 and 2.2 is shifted towards the H_2 production. Therefore, higher H_2 yields can be obtained at lower temperatures (723-873 K) with a simpler process layout. There is no need for water-gas shift reactors or absorption columns and also less demanding requirements for the reactor materials due to lower operating temperatures.

The main advantages of SESMR can be understood from a thermodynamic analysis of the involved reactions:

$$\text{Reforming}: \quad CH_4(g) + H_2O(g) \Longleftrightarrow CO(g) + 3H_2(g) \tag{2.3}$$

$$\text{WGS}: \quad CO(g) + H_2O(g) \Longleftrightarrow CO_2(g) + H_2(g) \tag{2.4}$$

$$CO_2 \text{ removal}: \quad MO(s) + CO_2(g) \Longleftrightarrow MCO_3(s) \tag{2.5}$$

$$\text{Overall}: \quad CH_4(g) + 2H_2O(g) + MO(s) \Longleftrightarrow MCO_3(s) + 4H_2(g) \tag{2.6}$$

where MO is typically a metal oxide that can selectively react with CO_2 forming a metal carbonate (MCO_3). Eventually, saturation of the CO_2 acceptor will occur and regeneration is necessary. Regeneration can be accomplished by temperature or pressure swing. If CO_2 capture is desired, the regeneration should be carried out in steam, CO_2, or a mixture of the two. Various metal oxides have been identified in literature for application in SESMR as CO_2

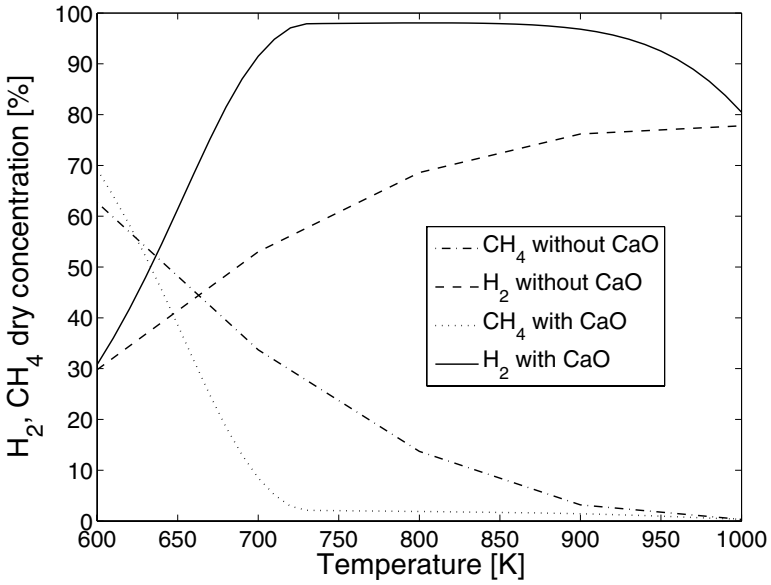

Figure 2.2: H_2 and CH_4 equilibrium concentrations at 1 bar, steam-to-carbon ratio of 3 and CaO to CH_4 ratio of 3 (calculated from FactSage [14]).

acceptors. An overview of high temperature CO_2 acceptors and their properties is given later in this chapter.

Figure 2.2 compares the H_2 and CH_4 equilibrium concentrations during SMR and SESMR operation at various temperatures, using CaO as CO_2 acceptor. It is observed that at such conditions (1 bar, S/C=3, CaO/CH_4=3), SESMR results in hydrogen yields close to 98% on dry basis at temperatures between 750 and 850 K. Only 60 to 75% H_2 can be obtained at similar conditions when the thermodynamic equilibrium is governed by SMR (without CaO). It should be mentioned that the main impurity during SESMR operation is unconverted CH_4 (about 2%, dry basis) with traces of CO and CO_2. The CO concentration depends strongly on the operation temperature due to the equilibrium of the WGS reaction. Harrison *et al.* have demonstrated that production of rich H_2 ($\geq$ 95%) containing less than 20 ppm CO is possible using CaO as CO_2 acceptor at 753 K and 5 bar [16]. In fact, Yi *et al.* were able to produce a product gas containing 96% H_2 with CO concentration near 50 ppm at atmospheric pressure and 733 K; suggesting the possibility of integrating SESMR with proton exchange membrane (PEM) fuel cells [17]. Operation at low temperatures and high pressure is beneficial to minimise the amount of

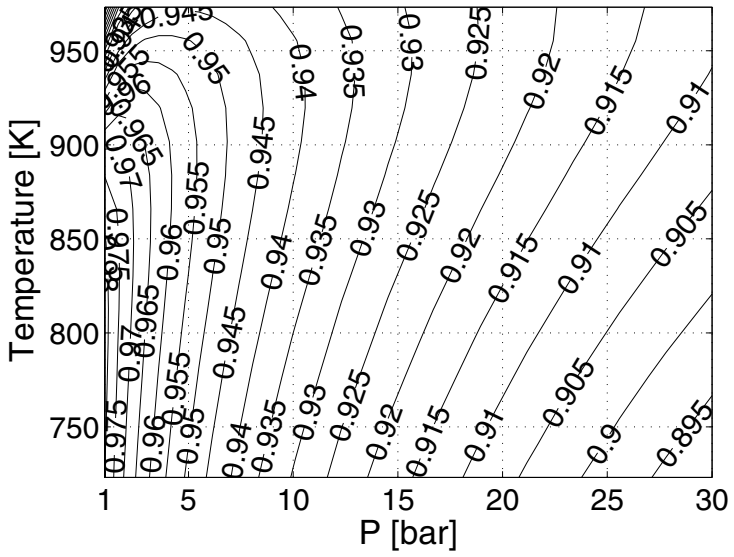

Figure 2.3: Thermodynamic simulation of the hydrogen yields obtained by application of SESMR when CaO is used as acceptor. S/C=3. The numbers stated in the figure are the mole fractions of hydrogen on a dry basis.

CO in the flue gas, due to more favourable equilibrium of reactions 2.4 and 2.5. However, as observed in Figure 2.3, these operation conditions will have a penalty in the H_2 yield because of the endothermic reforming reaction (reaction 2.3). Therefore, a tradeoff between temperature, pressure and S/C ratio is crucial and necessary in order to optimise the desired product composition.

2.2.2 SESMR literature overview

The concept of combining chemical reaction and separation of reaction products in a single unit operation is not new. The first reference to H_2 production combining a catalyst with a CO_2 acceptor was published in 1868 [18]. Later in 1933 and 1963, Williams [19] and Gorin and Retallick [20] issued respective patents for fixed-bed and fluidised-bed processes involving sorption-enhanced reaction. Natural limestone was selected as CO_2 acceptor in both processes. However, the process was not further developed at that time. It is during the last ten years that great interest has arisen again in the application of SESMR for H_2 production. The renewed interest is probably due to the continuous seeking for alternative routes for power generation and growing concern on

CO_2 emissions and global warming.

Different variations of the sorption-enhanced process can be found in the recent literature. These variations include the use of different CO_2 acceptors, raw materials, reactor conditions and reactor concepts. A group at the Louisiana State University has been working intensively in the demonstration of sorption-enhanced processes using CaO as CO_2 acceptor [11, 16, 17, 21–23]. Han and Harrison [21] experimentally demonstrated that high conversion of carbon monoxide to hydrogen, above the thermodynamic equilibrium, could be achieved in the absence of a catalyst by the sorption-enhanced water-gas shift reaction. The experiments were carried out in a fixed-bed reactor using natural dolomite as CO_2 acceptor. Some years later in the same group, Balasubramanian *et al.* [11] showed experimentally that fractions larger than 95% of H_2 (dry basis) could be produced in a single reactor containing reforming catalyst and CaO formed by calcination of commercial high-purity $CaCO_3$. Lopez *et al.* [23] confirmed these results using inexpensive commercial dolomite in a fixed-bed reactor. In addition, they studied the multi-cycle properties of the process. Regeneration of the spent acceptor was carried out in different atmospheres and temperatures from 1073 to 1223 K. They concluded that in all cases a continuous decrease in the fractional conversion of the acceptor existed, mainly due to the severe conditions required for the regeneration.

One of the main advantages of SESMR in addition to the high H_2 yields is the possibility of producing H_2 with small traces of CO. The Louisiana State University group has also studied in detail the best conditions for low-carbon monoxide hydrogen production by SESMR both at high pressures and atmospheric pressure [16, 17]. They concluded that production of high purity H_2 ($\geq$ 95%) with less than 20 ppm CO can be produced at 753 K, S/C=4, and 5 bar; while at 1 bar the amount of CO at similar conditions is near 50 ppm. These experiments were always carried out in a fixed-bed reactor using natural dolomite as acceptor. Recently, Hildenbrand *et al.* have pointed out that there exist some limitations in the use of CaO as CO_2 acceptor, mainly due to the formation of $Ca(OH)_2$ in the presence of high partial pressures of steam [24]. Although $Ca(OH)_2$ is also an effective CO_2 acceptor, hydration of CaO is not desired as the H_2O removed from the gas phase during hydrate formation reduces the steam-to-carbon ratio and the extent of the reforming reaction. Another associated problem with using natural sorbents as dolomite is that they usually contain sulphur, and a pretreatment of the acceptor will be necessary [23]. However, it is possible to find sulphur-free natural dolomites. Arctic Dolomite SHB has been successfully used as CO_2 acceptor for SESMR without

any preteatment by Johnsen *et al.* [25].

Figure 2.4 shows SESMR experimental results performed in our laboratories using Arctic SHB Dolomite. The effluent concentration profiles of both H_2 and CO_2 during successive cycles are presented. It is obvious from the figure that hydrogen yields over 98% could be achieved at these conditions (equilibrium: 98.4% H_2). After saturation of the acceptor, the breakthrough of the CO_2 takes place and the conversion of methane decreases following the thermodynamics of conventional steam methane reforming. Accordingly, the H_2 yield decreases to approximately 70.5% (equilibrium: 69.9% H_2). Successive cycles were carried out with intermediate regeneration at 1023 K in Ar. The H_2 yield was constant at 98% during all cycles, but earlier breakthrough was observed due to decay of the acceptor capacity.

All the experimental investigations mentioned so far have been carried out in small scale fixed-bed reactors. However, fixed-bed reactors might not be the best reactor configuration for SESMR processes where continuous regeneration of the acceptor is necessary. In fact, for continuous operation at least

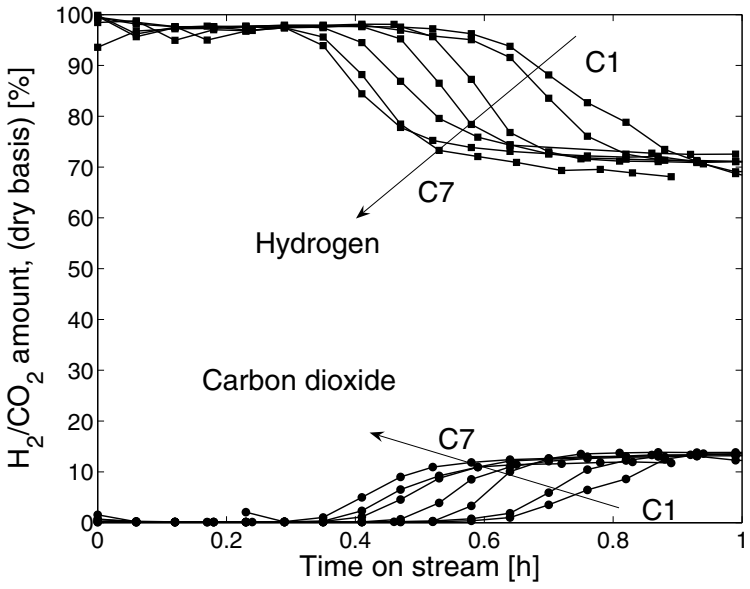

Figure 2.4: Effluent H_2 and CO_2 concentration profiles on a water free basis during successive cycles (C). 7.25 g calcined dolomite, 1.45 g Ni catalyst, 848 K, S/C=5, 5 bar, 47 ml/min CH_4. Regeneration: 1023 K in Ar.

two reactors need to be operated alternating from reforming to regeneration mode. Synchronisation of two reactors is challenging since there is normally a mismatch between capture and regeneration times. Johnsen [26] has recently proposed the alternative of using fluidised-bed reactors. Fluidised-beds introduce several interesting advantages such as: good mixing of solids, low pressure drop, good temperature control and transfer of particles between reactors, making continuous operation possible. Johnsen *et al.* have shown, both experimentally [25] and by modelling [27], that hydrogen equilibrium concentrations above 98% (dry basis) can be obtained carrying out SESMR in a bubbling fluidised-bed reactor using calcined dolomite as CO_2 acceptor at atmospheric pressure. However, these experiments were also carried out batchwise due to limitations in the reactor configuration that did not allow feeding of solids. In fact, the only experimental investigation that claims continuous production of H_2 by SESMR is based on two parallel fixed-bed reactors operated in a cyclic manner [28]. Reactor I (reforming) was operated at 903 K and S/C=5, while rector II (regeneration) was operated at 1123 K using Ar as a carrier gas. Therefore, the recovery of CO_2 was not considered. The authors used a self-made CaO based acceptor and claim continuous production of more than 90% H_2 (dry basis).

All the examples cited so far include the reaction of CO_2 with a metal oxide (CaO) forming a carbonate ($CaCO_3$). The total reforming reaction is at normal operation conditions close to authothermal. However, a large input of energy is required in order to regenerate the acceptors by a temperature swing process. Dupont *et al.* [29] have reported an interesting variation of the SESMR that allows operation close to authothermal conditions both during the reforming and regeneration. This process has been called unmixed steam reforming, and its principle relies on carrying the regeneration in an oxygen rich atmosphere. Under oxidative conditions the Ni catalyst present in the catalyst bed will oxidise, providing the heat necessary for the regeneration of the Ca based acceptor. Re-reduction will happen when contacting the catalyst with the fuel during the reforming step. This process is based in an earlier study of Lyon *et al.* [30] that proposed the unmixed combustion as an alternative to fire.

Air Products and Chemicals Inc. has also shown a large interest in the study of what they called sorption-enhanced reaction process (SERP) [15, 31–33]. The main difference with the processes described above is the use of a different kind of material as CO_2 acceptor. In this case, an acceptor that can adsorb CO_2 weakly is used, instead of an oxide that reacts chemically. Therefore, regeneration of the CO_2 adsorbent can be carried out efficiently by means of a pressure

swing process. They used a potassium carbonate promoted hydrotalcite and claimed direct production of high purity hydrogen ($\geq$ 95%) containing CH_4 as the bulk impurity (about 5%) and carbon oxides as trace impurities (50 ppm) [15]. Several experimental and theoretical studies have supported the SERP process in the last years [34–40].

Summarising, numerous reports have been published describing sorption-enhanced processes the last few years. It has been shown that SESMR is a flexible process that allows production of high purity hydrogen in a broad range of temperatures and pressures [11], reactor configurations [11, 25], and various fuels [21, 29, 41, 42]. Proper regeneration will also allow recovery of the CO_2. On the other hand, the selection of an appropriate CO_2 acceptor has a strong impact on the feasibility of SESMR. Criteria for selecting CO_2 acceptors and an overview over possible candidates are included in section 2.3.

2.2.3 Catalyst for SESMR

SMR is typically carried out using a Ni based catalyst. The catalyst must sustain severe operating conditions, including temperatures in the range 1023 to 1173 K and pressures up to 30 bar. In addition, it must have sufficient activity, resistance to coke formation and sintering, and high mechanical strength [43].

Typical reaction temperatures in SESMR are between 673 and 873 K, significantly lower than for SMR. The low working temperatures imply the need of a very active reforming catalyst. In addition, high steam-to-carbon ratio is also preferred in order to maximise the H_2 yield in SESMR. This may expose the catalyst to severe sintering conditions. Therefore, it is beneficial to develop a catalyst with optimum properties at these operation conditions.

It is generally agreed that the Ni crystallite size plays an important role in the reforming catalyst activity and stability. Wei *et al.* [44] have systematically studied the effect of metal dispersion and support on the forward CH_4 turnover rates of various noble catalysts and Ni. In all cases, CH_4 reforming turnover rates increased with increasing metal dispersion, but they were not influenced by the support. In addition, smaller Ni crystals are also known to be more resistant to carbon formation. Bengaard *et al.* [45] suggested that a minimum nucleus of graphene at a Ni step is needed before it is stable. The formation of this nucleus is slow and if the facets or step edges of Ni are too small nucleation might not proceed, and graphite formation is suppressed.

Other approaches proposed for reducing the risk of coke formation include

the use of Ni/Mg-Al catalysts that favour carbon gasification. One way of obtaining these catalysts is by thermal decomposition of synthetic hydrotalcite anionic clays [46, 47]. The use of synthetic hydrotalcites as catalyst support is also interesting due to the high surface area, basicity and nanocrystalline nature of the resulting oxides after thermal treatment [48]. Hydrotalcites are represented by the following formula:

$$[M_n^{2+}M_m^{3+}(OH)_{2(n+m)}]^{m+}A_{m/x}^{x-}.yH_2O \tag{2.7}$$

where M^{2+} and M^{3+} are metal cations, A is an anion, x the is charge of the anion, $n>m$ and y is the number of interlayer water molecules. The nature of the cations, the type of charge balancing anions, the amount of interlayer water and the size and morphology of clay particles can be varied to produce materials with specific properties. In addition, if the material is heat-treated the hydrotalcite structure is lost and the material becomes a mixture of oxides and mixed oxides. However, this material retains a memory effect which allows the reconstruction of the original structure under mild conditions when contacting the product of the thermal treatment with water solutions containing various anions.

There exist several investigations related to Ni-based hydrotalcite-like catalysts. Clause *et al.* [47] confirmed that hydrotalcite-like anionic clays resulted in formation of small and stable NiO particles with high surface area, even at high Ni loadings. However, the reducibility of the oxides can be low if calcination is carried out at temperatures above 1023 K, due to the formation of spinels [49]. Takehira *et al.* [50] used Ni catalysts prepared from a Mg-Al hydrotalcite-like anionic clay in steam reforming of CH_4 and compared their behaviour with other catalyst prepared by impregnation. They concluded that the catalyst derived from hydrotalcite-like compounds had a higher activity and showed no deterioration after 600 h on stream at a low steam-to-carbon ratio (S/C=1.6).

It is believed that the benefits of using hydrotalcite-derived oxide mixtures are due to the strong interaction between the support and nickel. This results in smaller Ni crystals with excellent stability and high activity in steam reforming of methane. In addition, preparation of high loaded catalyst is possible by this route. Therefore, such catalysts are considered interesting for application in SESMR.

2.3 High temperature solid CO_2 acceptors

2.3.1 Requirements

The selection of an appropriate CO_2 acceptor for application in SESMR is not straightforward and several requirements have to be fulfilled. Firstly, the acceptor should have a large CO_2 sorption capacity and high reaction rates for both capture and regeneration. In addition, thermal, mechanical and long term multi-cycle stability are also required. On the other hand, SESMR is a batch process that requires regeneration of the acceptor after saturation with CO_2. Regeneration can be carried out by temperature swing or pressure swing depending on the nature of the acceptor. In the case of a temperature swing process, a small temperature gap between capture and regeneration is desired in order to minimise the energy loss.

2.3.2 Candidates

There has been an extensive research on the uptake of CO_2 on acceptors at ambient temperature and atmospheric pressure. However, there are fewer relevant investigations about the capture of CO_2 at high temperatures and pressures [51]. Different materials have been proposed in literature that can take CO_2 at moderate temperatures (298-523 K). For example, Yong *et al.* [52] have reported that carbon based sorbents have adequate capacity for CO_2 at relatively low temperatures (298-523 K). The capture capacity of these materials is reduced when the capture temperature is further increased (>523 K). Different zeolites have also been reported to work in the same range of temperatures [53]. However, these temperatures are still too low for application in SESMR. In fact, acceptors which can selectively remove CO_2 from the SMR reaction zone at temperatures above 673 K are desirable. The acceptors that have been mostly investigated in the literature for application in SESMR include the natural sorbents limestone and dolomite, and hydrotalcite-like compounds (HTlc).

Hydrotalcite-like compounds (HTlc)

Hydrotalcite-like compounds belong to a large class of anionic and basic clays, also known as layered double hydroxides. A typical composition of this layered double hydroxide is $Mg_6Al_2(CO_3)(OH)_{16} \cdot 4H_2O$. These materials can chemisorb CO_2 at temperatures typically between 673 and 773 K, mainly due to the strong basic sites at the surface of the structure [40]. Ding *et al.* [54] studied the equilibrium and kinetics of CO_2 capture on potassium promoted

hydrotalcites. They concluded that the adsorption capacity of HTlc is low under dry conditions (0.65 mol CO_2/kg at 673 K [54]). An enhancement in the capacity of approximately 10% was observed when operating in wet feed conditions independently of the amount of water. Similar results were also found by Yong *et al.* [55, 56]. In addition to low capacity, the adsorbent suffers a relatively rapid degradation during multi-cycle operation [54–56]. This deactivation, together with low capacity might make the application of such materials in an industrial scale difficult. However, a great scientific interest is still shown on hydrotalcite-based CO_2 acceptors [57–61].

Dolomite and limestone

Several researchers have studied the use of CaO precursors such as limestone and dolomite as CO_2 acceptors. Limestone and dolomite are both sedimentary rocks composed largely of the mineral calcite (calcium carbonate: $CaCO_3$) and calcium magnesium carbonate ($CaMg(CO_3)_2$), respectively. Calcination of limestone results in CaO with a stoichiometric capacity of 0.79 g CO_2/g acceptor, while calcination of dolomite results in a mixture of CaO-MgO. It has been shown that MgO does not participate in the CO_2 removal and stays inert after calcination. Therefore, the stoichiometric capacity of dolomites is 0.46 g CO_2/g acceptor.

There exist many studies on the carbonation reaction of such acceptors [22, 62–64]. They all agree that the CO_2 capture happens in two different steps: after a rapid, chemically controlled initial carbonation period, a much slower second stage is reached, which strongly limits the carbonation conversions. This change in the reaction rate is attributed to the formation of a $CaCO_3$ product layer surrounding the CaO. When this layer reaches a certain thickness, the carbonation of the inner core is severely hampered. Alvarez *et al.* [65] have estimated a critical product layer thickness of around 50 nm that seems to be acceptable to a wide range of limestones and working conditions.

The main problem associated with Ca based natural acceptors is the rapid decay observed in their maximum capacity during many carbonation/calcination cycles [26, 64, 66, 67]. Abanades *et al.* [66] studied the conversion limits in the reaction of CO_2 with limestone and compared them with published work by other authors. They concluded that there is an unavoidable decay in activity that depends almost exclusively on the number of operating cycles. They explain this decay in terms of loss of porosity associated with small pores and a certain increase of the porosity associated to large pores. According to Grasa *et al.* [67], the capture capacity of limestones decreases dramatically in the first

20 cycles and tends to stabilise after successive cycles to a residual conversion of 8% that remains nearly constant after 500 cycles.

However, although limestone has a greater CO_2 capacity per unit mass than dolomite, dolomite has been shown to be a superior sorbent in other respects, as the multi-cycle performance [21, 22]. The reason that makes dolomites more stable than limestone may be the presence of inactive MgO that does not take part in the carbonation reaction and thus, partially hinders the sintering inside the CaO particle during calcination [68].

Johnsen [26] has evaluated the multi-cycle sorption properties of Arctic Dolomite at different exposure times, degree of carbonation and atmospheres. It is observed than degradation of the acceptor happens at all conditions and depends strongly on the total exposure time at elevated calcination temperatures. However, the decay can be controlled to an extent. For example, incomplete carbonation of the acceptor during cycling operation, or calcination in a mixture of water and nitrogen, resulted in significantly improved stability.

CaO synthetic acceptors

Nowadays, several efforts are being done in order to overcome the losses in capacity of natural calcium-based acceptors [68–70]. Li *et al.* have claimed that they are able to synthesise a CaO based acceptor with a capacity of 0.45 g CO_2/g acceptor that do not degrade upon multi-cycle test with calcination under mild conditions [68, 69]. The acceptor consists of CaO (75%) supported on $Ca_{12}Al_{14}O_{33}$ (25%). Similarly, Feng *et al.* have reported that CaO supported on γ-Al_2O_3 did not show loss in capacity after nine cycles, and reached a degree of reaction higher than 90% [70]. However, because the content of CaO was relatively low (4.3%), the overall capacity of the absorbent is low.

Ceramic acceptors

Li and Na metal oxides have been recently reported as very good candidates for the CO_2 removal with high capacity and stability [12, 71–84]. Examples of these materials are shown in the next reactions:

$$Li_2ZrO_3 + CO_2 \Longleftrightarrow Li_2CO_3 + ZrO_2 \quad \Delta H^0_{298} = -160 \text{ kJ/mol} \tag{2.8}$$

$$Na_2ZrO_3 + CO_2 \Longleftrightarrow Na_2CO_3 + ZrO_2 \quad \Delta H^0_{298} = -149 \text{ kJ/mol} \tag{2.9}$$

$$Li_4SiO_4 + CO_2 \Longleftrightarrow Li_2CO_3 + Li_2SiO_3 \quad \Delta H^0_{298} = -143 \text{ kJ/mol} \tag{2.10}$$

Nakagawa *et al.* reported for first time in 1998 that lithium zirconate can efficiently hold CO_2 in amounts up to 28.8 acceptor weight percent at temperatures between 723-873 K according to the reversible reaction 2.8 [12]. Just one year later, Ohashi and Nakagawa [71] found out that the properties of Li_2ZrO_3 could be improved by doping the mixed oxide with K_2CO_3. Promoting Li_2ZrO_3 with K_2CO_3 increases the carbonation rate because of the formation of an eutectic molten carbonate composed of Li_2CO_3 and K_2CO_3 at high temperatures. This molten carbonate can significantly enhance CO_2 diffusion compared to the solid shell in pure Li_2ZrO_3.

Kato and Nakagawa [72] proposed the use of a new lithium containing oxide, Li_4SiO_4, that can take CO_2 in amounts up to 36.6 acceptor weight percent in a similar range of temperatures than Li_2ZrO_3 (reaction 2.10). They showed that Li_4SiO_4 was a better candidate since it can absorb larger amounts of CO_2 and with faster kinetics. Kato *et al.* claimed that Li_4SiO_4 can absorb CO_2 with a reaction rate about 30 times faster than Li_2ZrO_3 at 773 K in an atmosphere of 20% CO_2 [85]. In addition, Li_4SiO_4 can absorb CO_2 at much lower concentrations even at room temperature.

Recently, sodium-based acceptors, such as Na_2ZrO_3, have been reported as good alternatives for Li_2ZrO_3 and Li_4SiO_4. López-Ortiz *et al.* [78] compared the uptake rates of the three materials at 873 K and 100% CO_2, and found that Na_2ZrO_3 had the most favourable kinetics.

From a thermodynamic point of view, all the variations of alkaline acceptors show reasonable favourable equilibrium for CO_2. Figure 2.5 shows the equilibrium partial pressures of carbon dioxide for CaO and the ceramic acceptors shown here, in the temperature interval from 725 to 1000 K. CaO shows more favourable thermodynamics than the Li and Na based mixed oxides. Accordingly, CaO can remove lower concentrations of CO_2. Li_2ZrO_3 and Na_2ZrO_3 show very similar equilibrium concentrations, with Li_4SiO_4 being the less favourable. It should be noticed that doping Li_2ZrO_3 with K can enhance the CO_2 equilibrium. However, the more favourable the capture reaction is, higher temperatures are required for regeneration. Temperatures above 1173 K are needed for regeneration of CaO in pure CO_2. This temperature is high if compared to the respective temperatures for the ceramic acceptors: 990 K, 1020 K and 1050 K for Li_4SiO_4, Li_2ZrO_3, and Na_2ZrO_3, respectively. Table 2.1 summarises the main properties of the most commonly used CO_2 acceptors.

The relatively high capture capacity, stability and lower regeneration temperatures of ceramic acceptors make them promising for application in both pre-

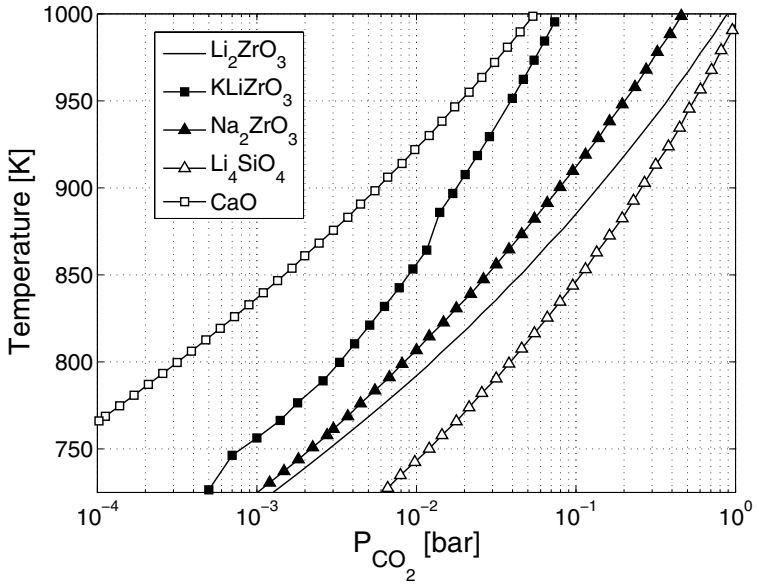

Figure 2.5: Equilibrium partial pressures of carbon dioxide as a function of temperature for the different acceptors.

Table 2.1: Properties of various high temperature CO_2 acceptors.

Acceptor	Capacity [g CO_2/g]	Stability	Kinetics	Regeneration temperature[a] [K]
Dolomite	0.46	Poor	Good	1173
Limestone	0.79	Poor	Good	1173
$CaO/Ca_{12}Al_{14}O_{33}$	0.45[b]	Fair	—	1173
CaO/γ-Al_2O_3	0.033[c]	Good	—	1173
Li_2ZrO_3	0.29	Fair	Fair/Poor	1020
Na_2ZrO_3	0.24	Fair	Good	1050
Li_4SiO_4	0.36	Fair	Fair	990
Hydrotalcite	0.029[d]	Fair/Poor	Good	PSR[e]

[a] Equilibrium regeneration temperature at 1 bar and 100% CO_2 [14]
[b] Capacity reported by Li *et al.* [68]
[c] Capacity reported by Feng *et al.* (4.6% CaO, 90% reacted) [70]
[d] Capacity reported by Ding *et al.* (0.65 mol CO_2/kg) [34]
[e] PSR: pressure swing regeneration

and post-combustion systems. However, kinetic limitations during the CO_2 capture, specially for Li_2ZrO_3, are still the main obstacle for application in processes as such SESMR [86].

The synthesis of lithium containing ceramic powders has been extensively studied, in particular lithium zirconate since it is one of the candidates of the tritium breeding for nuclear fusion reactors [87–90]. Various solid state processes have been employed to fabricate the lithium zirconate powders. Solid state reactions between ZrO_2 and lithium peroxide (or carbonate) are the best known processes [12, 72, 87]. In these processes, two types of powders are mechanically mixed and treated at high temperatures. Solid state reactions normally require high temperatures and long reaction times. For example, Ida *et al.* [74] prepared pure Li_2ZrO_3 powder having particle diameters larger than 1 μm by solid state reaction of Li_2CO_3 and ZrO_2. The final particle size of the powder prepared by solid state methods is normally large, partially due to sintering during the high temperature treatment. The particle size is also controlled by the particle size of the starting ZrO_2.

There have been several efforts to reduce the starting powder size for solid state processes. One example is the use of a sol-gel technique to prepare fine powders of ZrO_2 [77]. However, this powder is subsequently reacted in solid state with Li_2CO_3 at high temperatures with following sintering problems. A precipitation combustion process has also been reported to synthesise Li_2ZrO_3 powder as breeding material for fusion reactors [88]. Li_2ZrO_3 can easily be obtained by this method using a mixture of urea and citric acid in stoichiometric composition. The primary particle size of these powders was smaller than 20 nm. However, the powder contains impurities and requires high calcination temperatures. There are other wet-chemistry routes reported for the preparation of Li_2ZrO_3 as a breeding material. Alvani *et al.* developed two wet routes starting from metal alkoxides where temperatures higher than 1073 K were required for the preparation of Li_2ZrO_3 [87]. Montanaro *et al.* proposed a gelling method using lithium acetate and zirconium propylate as precursors [89]. However, this method yielded particle sizes larger than 40 μm. Unfortunately, most of these synthesis routes were used to prepare Li_2ZrO_3 for other applications than CO_2 acceptor, and no data on CO_2 uptake kinetics, capacity or regeneration is available.

Recently, Nair *et al.* have done a systematic study on the properties of Li_2ZrO_3 with different crystal structures as CO_2 acceptors [77]. They have compared the properties of powders prepared by solid state reactions of mixed powders,

sol-gel prepared powders and commercial grade powder. Their results indicated that tetragonal Li_2ZrO_3 powders show a larger rate of sorption than their monoclinic counterparts. They also concluded that small particle size is critical to enhance the CO_2 capture. The same conclusion was recently reached by Yi *et al.* after preparing tetragonal Li_2ZrO_3 by a low temperature liquid state synthesis [83].

2.3.3 State of the art

Most of the studies on high temperature CO_2 acceptors are related to the use of the natural CaO precursors dolomite and limestone. CaO shows good uptake kinetics and the most favourable thermodynamics. However, these compounds suffer from a large decay in their capacity after several cycles. The regeneration of Ca-based acceptors is highly energy demanding. The use of high temperatures for the regeneration leads to sintering and subsequent pore blockage and losses in the porosity.

Several efforts are being done in order to overcome the losses in capacity of calcium-based acceptors. Preliminary results using a carrier to support the synthetic CaO are very promising.

As an alternative, the application of ceramic materials such as CO_2 acceptors have been discussed extensively. However, there are still some open questions related to their durability, regeneration conditions, effect of steam and uptake kinetics. In fact, Abanades *et al.* have claimed that Li based materials must sustain several thousand cycles in order to compete with the inexpensive acceptors dolomite and limestone [91]. Therefore, there is a need to study in detail the properties of alkaline based acceptors and their performance at SESMR conditions.

Chapter 3

Experimental

The objective of this chapter is to provide a short description of the experimental procedures followed for synthesis of materials, characterisation techniques, and reaction testing.

3.1 Synthesis

3.1.1 Synthesis of pure and potassium promoted Li_2ZrO_3

Zirconyl nitrate ($ZrO(NO_3)_2 \cdot x\ H_2O$) and lithium acetate ($CH_3COOLi \cdot 2H_2O$) were used as precursors for preparation of pure nanocrystalline tetragonal Li_2ZrO_3. Appropriate amounts of each precursor were dissolved in deionised water. After standardisation of the solutions by thermogravimetric analysis, the precursors were mixed for several hours in appropriate amounts to form a complex solution. Drying of the solution was carried by two different routes. In some cases, the solution was spray dried (Büchi, Mini Spray-Drier B-191) with an input temperature of 423 K and a pump rate of 2 ml/min. As an alternative drying route to the spray drying, the precursor solution was solidified by heating to 373 K in an oil bath under continuous stirring. The resulting solid products were further decomposed/oxidised in a certain temperature range, forming powders with homogeneous atomic mixture of Li and Zr. The powders were calcined at 873 K in air, leading to decomposition of the organic compounds by a smouldering reaction.

Non stoichiometric Li_2ZrO_3 samples were also prepared according to this procedure. The sole difference was the ratio between the two starting precursors.

Li:Zr molar ratios equal to 1.8 and 2.2 were used resulting in $Li_{1.8}ZrO_{2.9}$ and $Li_{2.2}ZrO_{3.1}$, respectively.

The preparation of potassium doped samples was similar to the procedure described above, although potassium carbonate (K_2CO_3) was added as K precursor. Defined amounts of the three precursor solutions were mixed, dried and calcined at identical conditions as earlier described. A series of potassium doped samples were prepared by varying the K:Li:Zr ratio.

3.1.2 Synthesis of Na_2ZrO_3

Sodium citrate (NaCA) and zirconyl nitrate ($ZrO(NO_3)_2 \cdot xH_2O$) were used as precursors for preparation of nanocrystalline monoclinic Na_2ZrO_3. Appropriate amounts of each precursor were dissolved in deionised water and mixed under vigorous agitation for 3 h. The Na/Zr molar ratio used for the synthesis of sodium zirconate was 2.0. The resulting solution was evaporated under continuous stirring at 363 K overnight, leading to the formation of an amorphous zirconium complex. Then, this complex was placed in an alumina crucible and heat-treated in a muffle oven with a defined temperature program and gas atmosphere. The amorphous zirconium complex was heated from room temperature to 1073 K at 10 K/min under argon flow, and later calcined at this temperature for 3 h in air.

3.1.3 Synthesis of hydrotalcite-based Ni catalyst

A series of hydrotalcite-based Ni catalysts were prepared by co-precipitation of $Mg(NO_3)_2 \cdot 6H_2O$, $Al(NO_3)_3 \cdot 9H_2O$ and $Ni(NO_3)_2 \cdot 6H_2O$ to obtain 12.5 wt%, 40 wt% and 77.5 wt% Ni, respectively. The samples were prepared according to the following procedure. A three-neck vessel (1 l) equipped with a thermometer, a reflux condenser, and a mechanical stirrer was charged with 400 ml deionised water and calculated amounts of Na_2CO_3 and NaOH. A second solution containing calculated amounts of the Ni, Mg and Al precursor salts and 400 ml of deionised water was prepared. The second solution was added dropwise to the first solution while stirring for a period of about 2 h. After the addition was completed, the pH of the mixture was adjusted to between 8 and 9 adding small amounts a concentrated acid. Later, the mixture was heated for 15 h at 353 K. The resultant gel was cooled, filtered and thoroughly washed. The catalysts were dried overnight under vacuum at 343 K and calcined in air at 873 K for 6 h after being heated at a rate of 5 K/min. An additional sample was prepared by incipient wetness impregnation of $Ni(NO_3)_2 \cdot 6H_2O$ on HT70,

a commercial hydrotalcite support from Condea with $MgO/Al_2O_3 = 70/30$. The support was impregnated with nickel nitrate hexahydrate to obtain 12.5 wt% nickel. The catalyst was dried for 16 h at 373 K and calcined at the same conditions as the other catalysts.

3.2 Characterisation of materials

3.2.1 X-ray diffraction

X-ray diffraction (XRD) patterns were recorded at room temperature on a Siemens D5005 X-ray diffractometer using CuKα radiation ($\lambda = 1.54$ Å). The X-ray tube voltage was set to 40 kV and the current to 50 mA. The scans were typically recorded in the 2θ range between 20 and 85° using a step size of 0.03°. Peaks were identified by comparison with standards in a database [92].

The average crystallite thickness was calculated applying the Scherrer equation [93] on the most intense diffraction peak of the studied samples. The Scherrer equation [93] relates line width to crystal size:

$$< L >= \frac{K\lambda}{\beta \cos\theta} \tag{3.1}$$

where $< L >$ is a measure for the dimension of the crystallite thickness in the direction perpendicular to the reflecting plane, λ is the X-ray wavelength, β is the peak width, θ is the angle between the beam and the normal on the reflecting plane, and K is a constant.

Prior to calculations, the contribution of CuKα_2 radiation to the diffractogram was stripped using the computer software "DIFFRAC^{plus}" by Bruker AXS Inc. [92]. In addition, lanthanum hexaboride, LaB_6, was used as reference material to determine the instrumental line broadening. LaB_6 does not exhibit any broadening due to crystallite size or strain.

In situ high-temperature X-ray diffraction (*in situ* HTXRD) using a Siemens D5005 diffractometer equipped with a position sensitive detector (PSD-50M, MBRAUN) was carried out for the sample Li_2ZrO_3. The powders were dispersed in ethanol and applied on a platinum strip located in a high-temperature camera (HTK16, Anton Paar GmbH). The data were collected with a step size of 0.0364° and a step time of 0.5 s. The capture reaction was carried out at 848 K under a CO_2 containing atmosphere. The regeneration was carried out at 943 K under a flow of nitrogen. Scans were recorded every 10 min.

3.2.2 Nitrogen adsorption

Nitrogen adsorption-desorption isotherms of the CO_2 acceptors were measured with a Micromeritics TriStar 3000 instrument, and the data were collected at liquid nitrogen temperature, 77 K. The samples were outgassed at 573 K overnight prior to measurement. The surface area was calculated from the Brunauer-Emmett-Teller (BET) equation [94], while the total pore volume and the average pore size were calculated applying the Barrett-Joyner-Halenda (BJH) method [95].

The BET surface area of the Ni catalysts was measured by N_2 adsorption at 77 K in a CoulterTM SA 3100. Prior to the measurements, the samples were dried under vacuum at 423 K for 1 h.

3.2.3 Mercury porosimetry

Pore size measurements of Li_2ZrO_3 and Na_2ZrO_3 were also performed using a Carlo Erba Porosimeter 2000 by mercury intrusion. Each sample was evacuated and dried at 423 K prior to analysis. A cylindrical pore model was assumed.

3.2.4 Hydrogen chemisorption

H_2 adsorption isotherms of the Ni catalysts were measured at 308 K on a Micromeritics ASAP 2010C apparatus. The catalyst was loaded in a U-shaped quartz reactor heated by an electrical furnace. The samples were initially evacuated at 308 K for one hour, and after reduced in flowing H_2 at 943 K for 10 h (heating rate 2 K/min). After reduction, the samples were evacuated for 30 min at 943 K, and evacuated for 60 min at 308 K. An adsorption isotherm was constructed at 308 K based on the adsorbed amount of hydrogen at 10 different pressures in the range 4-310 mmHg. After evacuation for 30 min, a second isotherm was measured in order to separate strongly and weakly bonded H_2. The difference between the two isotherms represents the chemisorbed amount of H_2. The monolayer capacity was determined by extrapolating the linear part of the different isotherm to zero pressure.

The nickel dispersion was calculated from Equation (3.2):

$$D = \frac{AU}{\nu W} \tag{3.2}$$

where W is the weight fraction of Ni in the catalyst, A its atomic weight (58.69 g/mol), U is the amount of gas consumed and ν is the stoichiometry of the reaction (*i.e.* the number of gaseous molecules reacting per surface atom of the metal). It was assumed that two nickel surface atoms were covered by one hydrogen molecule (ν=1/2).

The dispersion, D, is directly related to the particle size from Equation (3.3):

$$D = \frac{fA}{\rho\sigma N_A} \cdot \frac{S}{V} \tag{3.3}$$

where ρ the specific mass (or density) of the Ni ($8.9 \cdot 10^{-21}$ g/nm^3), σ the average surface area occupied by one active Ni atom at the surface (0.065 nm^2), N_A is Avogadro's number ($6.022 \cdot 10^{23}$ mol^{-1}), and f is the fraction of the surface of the active phase which is effectively exposed to the reactants during the catalytic reaction. It was assumed that f=1.

From the above formula, assuming that all particles were identical spheres of diameter d, ($\frac{S}{V}$=$\frac{6}{d}$), Equation (3.3) can be expressed as:

$$d(\text{nm}) = \frac{101}{D(\%)} \tag{3.4}$$

3.2.5 Temperature programmed reduction

Temperature programmed reduction (TPR) of the Ni catalyst was performed in an in-house built equipment [96]. The catalyst was loaded in a U-shaped quartz reactor heated by an electrical furnace. The experiments involved heating of 0.2 g catalyst at a rate of 10 K/min to 1173 K in 7% H_2 in Ar. The gas flow rate was 30 ml/min.

The H_2 consumption was measured by analysing the effluent gas with a thermal conductivity detector (Shimadzu GC-8A gas chromatograph). The steam formed during the reduction was removed by a cold trap consisting of 2-propanol and dry ice.

3.2.6 Transmission electron microscopy

A scanning transmission electron microscopy (STEM) study was carried out on selected samples in a JEOL 2010F high resolution transmission electron

microscope. Images were recorded using the annular dark field signal which gives contrast that increases with atomic number. STEM specimens were prepared by ultrasonic dispersion of the lightly ground catalyst samples in ethanol, followed by allowing a drop of the suspension to dry on a holey carbon film supported by a copper grid.

3.2.7 Scanning electron microscopy

The morphology of Li_2ZrO_3 and Na_2ZrO_3 powders was examined in a Hitachi S-4300se field emission scanning electron microscope (FESEM) equipped with a field emission gun with Schottky emitter. The acceleration voltage was set to 5 kV and the secondary electron detector was used. STEM specimens were prepared by dropping some fine powder onto a wet carbon tape. The samples were also coated with a fine layer of carbon to enhance their conductivity.

3.2.8 X-ray photoelectron spectroscopy

The X-ray photoelectron spectroscopy (XPS) experiments were performed in an ultra-high-vacuum system with a base pressure of about 10^{-10} mbar. The measurements were performed using a SES2002 electron energy analyzer from Gammadata-Scienta, in conjunction with a monochromatised Al Kα ($h\mu$ = 1487 eV) X-ray source. A total resolution of about 0.7 eV was obtained for the XPS. The samples were prepared by dropping the fine powder onto a wet carbon tape.

3.3 CO_2 capture/regeneration measurements

CO_2 capture properties were evaluated using a tapered element oscillating microbalance (TEOM). The TEOM is produced by Rupprecht and Patashnick Co., Albany. A schematic drawing of the apparatus is given in Figure 3.1 [97, 98]. The TEOM consists of a hollow tapered quartz tube with a material test-bed in the narrow end. The internal volume is 0.17 ml. The tapered element is about 16 cm long, with an inner diameter of 4 mm and an outer diameter of 6 mm. During experiments, the tapered element was loaded with 20-30 mg of CO_2 acceptor together with quartz particles and kept in place with quartz wool and a metal cup.

The measurement of the mass change in the sample bed is based on changes in the natural frequency of the oscillating quartz element containing the sample. The main advantage of the TEOM is that all the gases are forced to flow

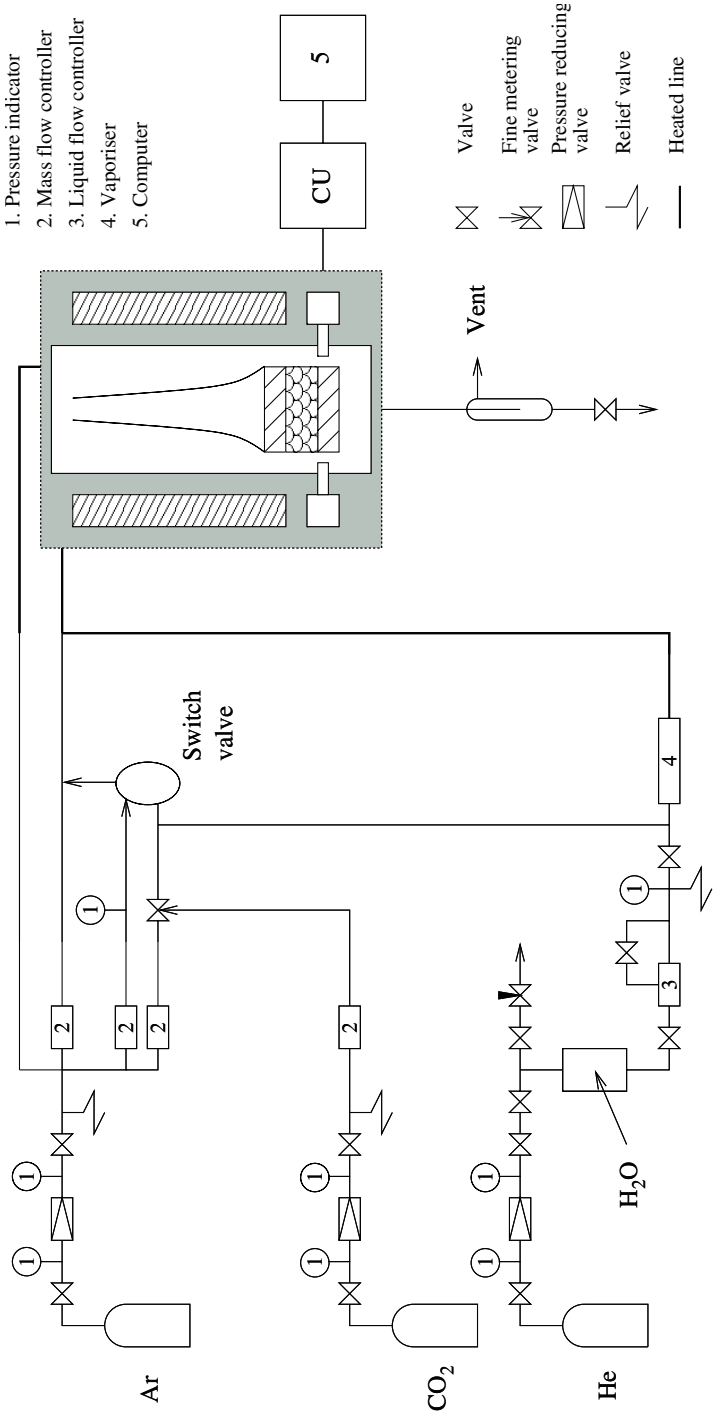

Figure 3.1: Schematic presentation of the tapered element oscillating microbalance reactor setup.

through the catalyst bed, avoiding the by-pass problem associated with a conventional microbalance. Thus, the sample bed can be treated as a fixed-bed reactor, and operation under differential conditions can be easily realised [97]. Other advantages of the TEOM compared to a conventional microbalance include:

- Direct, real-time mass change measurements
- High flow rates and better control of gas-solid contact
- Good time resolution: 0.1 s
- 1 μg mass sensitivity
- Capability of working at pressures up to 50 bar

An illustration of the experimental procedure used for screening the CO_2 capture and regeneration kinetics of the different acceptors is given in Figure 3.2. The extent of reaction is plotted versus the capture time. The extent of reaction, x, is defined as $x = \frac{\Delta\omega}{\Delta\omega_{max}}$, where $\Delta\omega$ and $\Delta\omega_{max}$ are the measured and the maximum experimental uptake of CO_2, respectively.

- Period A: the sample was heated to the capture temperature (T_c) in 100 ml/min of Ar with a heating rate of 10 K/min. The maximum operating temperature for the TEOM reactor is 953 K.
- Period B: the sample was kept at T_c under Ar atmosphere for stabilisation of the weight.
- Period C: the Ar atmosphere is switched to the reaction mixture at a time t_0. The different partial pressures of CO_2 in the reaction mixture were obtained by adjusting the flow rates of Ar and CO_2 at a total flow rate of 100 ml/min. This period is finished when no further increase in the extent of the reaction is observed. At this time, t_s, the acceptor is saturated.
- Period D: the reaction atmosphere is changed from the reaction mixture to pure Ar at a constant flow rate of 100 ml/min. In order to proceed with the regeneration of the acceptor, the temperature of the reactor is also increased from T_c to T_r (regeneration temperature) with a heating rate of 10 K/min.

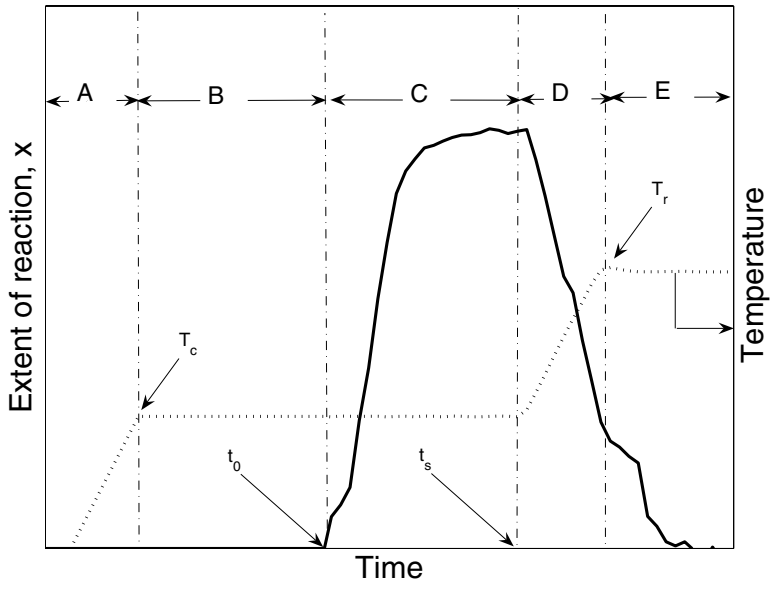

Figure 3.2: Scheme of the general procedure followed for the testing of the CO_2 capture properties of the prepared acceptors.

- Period E: the reaction temperature is kept at T_r until the sample is completely regenerated.
- After period E a new cycle was performed.

The experiments were carried out at different CO_2 partial pressures and capture/regeneration temperatures.

Due to the operating principle of TEOM, the mass of the gas occupied in the void volume in the tapered element affects the vibrational frequency of the balance. A mass change is detected when switching from one gas to another at isothermal conditions. This mass change is proportional to the density difference between the two gases according to Equation 3.5:

$$\Delta m = \frac{V_e P(M_2 - M_1)}{RT} \tag{3.5}$$

where M_2 is the average molecular weight of the feed mixture (CO_2/Ar mixture in this study), M_2 is the molecular weight of the inert gas (Ar), Δm is the

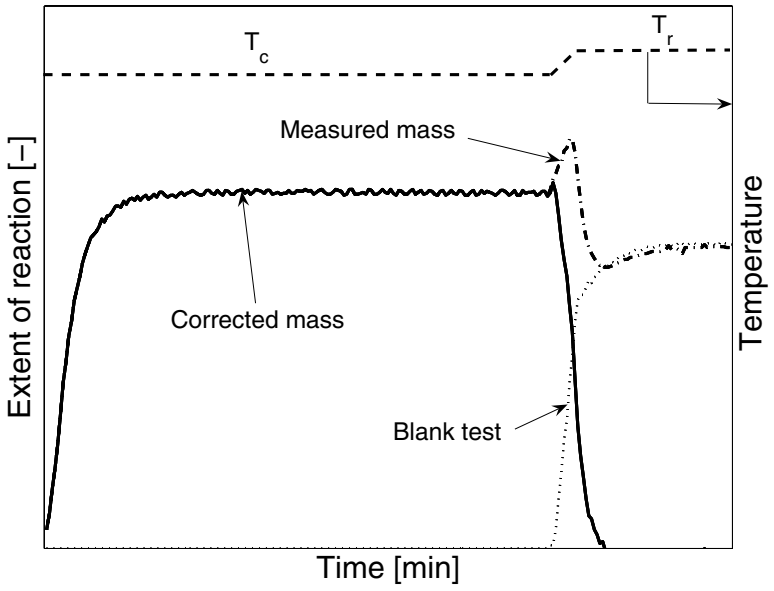

Figure 3.3: Scheme of the general procedure followed for the correction of non isothermal density change.

measured mass change, V_e is the void volume in the tapered element, T is the temperature, P is the pressure and R is the ideal gas constant. The void volume of the tapered element is approximately 1 ml and the molecular weight difference between the two switching gases (CO_2 and Ar) is very small. Thus, the mass change related to the density change in this system was always measured in the range 10^{-5}-10^{-6} g at the operation conditions. These values are negligible compared to the total mass change during the capture reaction and consequently no corrections related to the density change were necessary during the isothermal operation.

However, a temperature programmed process is carried out during the regeneration step. In this case the recorded apparent change on the mass is due to the release of CO_2 and changes in the reactor material properties, which result in changes on the vibrational frequency at different temperatures. A blank experiment is necessary in order to obtain the real mass change. An example is presented in Figure 3.3. The dash-dotted line represents the extent of reaction directly measured during a typical capture experiment. The starting and final points are at different temperatures and they cannot be directly compared. The dotted line represents a blank experiment, where the same

capture/regeneration cycle is repeated under inert atmosphere, with no CO_2 addition in this case. This cycle gives a direct indication of the mass change due to the temperature switch. Subtracting the blank experiment from the direct measurement gives the mass change due to the CO_2 release (solid line in Figure 3.3). All the regeneration curves showed in this study have been corrected according to this procedure.

3.4 Sorption-enhanced steam methane reforming

Sorption-enhanced steam methane reforming (SESMR) was run in a stainless-steel fixed-bed reactor with inner diameter of approximately 16 mm. A schematic illustration of the apparatus is given in Figure 3.4.

A mixture of Ni catalyst and CO_2 acceptor was introduced in the reactor without further dilution. Typical weight ratio between acceptor and catalyst was 5:1. The sample was held in the reactor by a stainless-steel grid and alumina wool. After the sample was loaded into the reactor, the system was flushed with Ar for one hour. The gas feed was controlled by digital mass flow controllers.

Prior to the reforming reaction, the sample was reduced at 1 bar and 943 K for 10 h under equal flow rates of H_2 and Ar (100 ml/min). A heating rate of 2 K/min was used to increase the temperature from ambient to 943 K. After reduction, the sample was cooled to 848 K in the same mixture.

The system was then pressurised to 5 bar in a mixture of H_2 and Ar. At 5 bar, the H_2 flow was decreased to 20 ml/min and water was introduced into the reactor system. Steam was generated by sending liquid water into a vaporiser kept at 673 K. The water flow was adjusted by a liquid flow controller. Helium was introduced in the water tank in order to degas and pressurise the deionised water prior to experiment. Typically 30-40 min were necessary until vapour water reached the reactor. Some H_2 was fed to the reactor in order to keep the catalyst in its reduced form.

At this point, the sorption-enhanced reforming reaction was started by simultaneously introducing methane into the reactor, closing the Ar feed and adjusting the water flow to reach the desired steam-to-carbon ratio. Typical reaction conditions were 848 K, 5 bar, steam-to-carbon ratio 5, acceptor-to-catalyst ratio 5 (250-500 μm) and total flow of 47 ml/min CH_4. The downstream gas composition was followed by an online Agilent microGC equipped with thermal conductivity detectors. Prior to analysis, the remaining water was removed in

a cold trap after the reactor and in an additional membrane just before the gas chromatograph.

The reaction was continued until the acceptor was saturated, which corresponded to the breakthrough of the CO_2 concentration in the product stream. At this point, the CH_4/steam mixture was switched to Ar (150 ml/min) and the temperature was increased for regeneration of the acceptor. Normally, 923 K for Li_2ZrO_3 and 1023 K for Na_2ZrO_3.

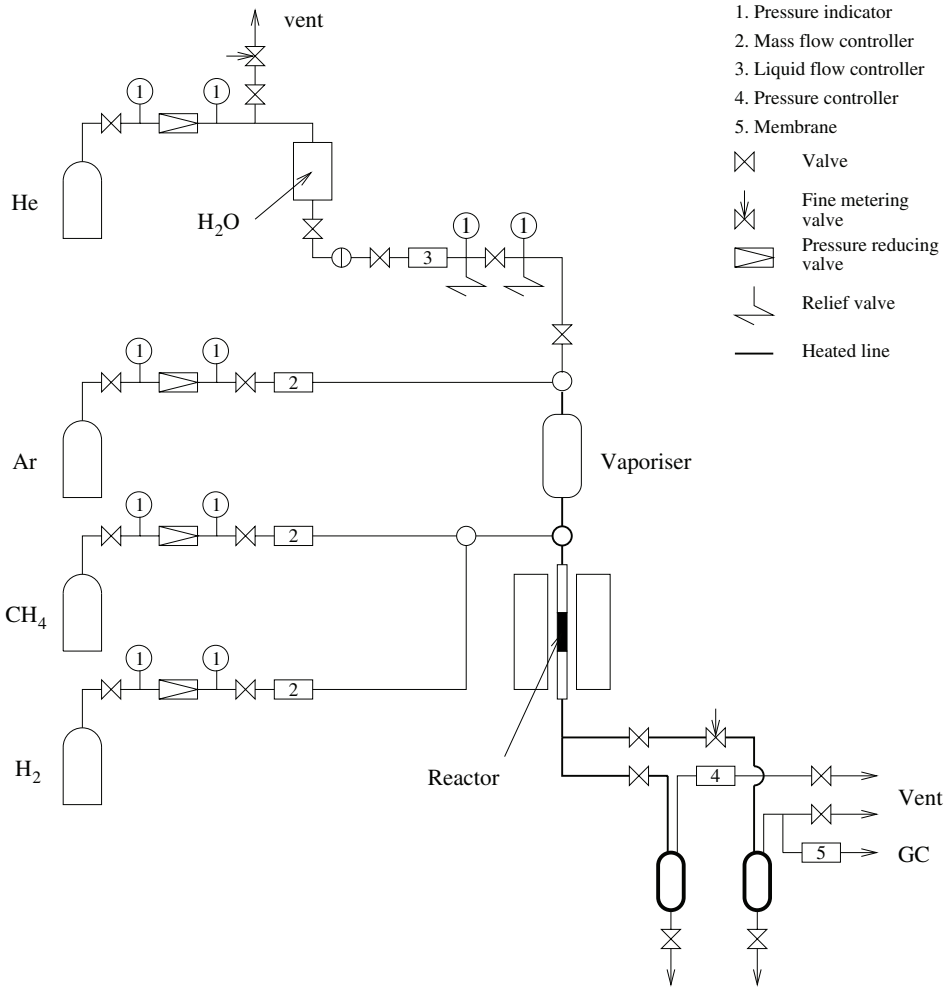

Figure 3.4: Schematic illustration of the sorption-enhanced steam methane reforming setup.

Multi-cycle experiments were carried out in order to study the stability of the system. Therefore, after regeneration the temperature was decreased to 848 K following the same procedure described earlier.

3.5 Steam methane reforming

The activity and stability of a series of Ni catalysts was studied in the same reactor set-up as illustrated in Figure 3.4. A stainless-steel fixed-bed reactor with 7 mm inner diameter was used in this case.

The catalyst bed consisted of 10 mg of Ni catalyst (250-500 μm) diluted with inert α-Al_2O_3 (100 mg). The catalysts were reduced at the same conditions as described above: Heated from room temperature to 943 K at 2 K/min in a mixture of H_2 and Ar and held at these conditions for 10 h.

Stabilisation of the catalyst was carried out at atmospheric pressure under sintering conditions: 923 K, S/C=3, and 50 ml/min of CH_4. Ar and H_2 were used as diluents to obtain a total gas flow of 100 ml/min. Product concentrations were measured online with a gas chromatograph.

Chapter 4

Results and discussion

4.1 Paper I and II: Synthesis and properties of Li_2ZrO_3 as a CO_2 acceptor

Nanocrystalline tetragonal Li_2ZrO_3 was prepared by a novel soft-chemistry route instead of traditional solid-state reactions in order to improve the kinetic properties and stability of the material. This soft-chemistry route has been described in section 3.1.1 and works under milder conditions than those needed for a solid-state route, providing an opportunity to minimise the starting particle size of Li_2ZrO_3. As a result, the properties of the powders such as capture rate of CO_2 and regeneration temperature have been significantly improved.

It was shown that a calcination temperature of 873 K was sufficient for the formation of nanocrystals of tetragonal Li_2ZrO_3. A further increase in the calcination temperature to 1073 K led to the formation of a mixture of Li_2ZrO_3 polymorphs (mainly monoclinic) and significant sintering. Therefore, the calcination temperature was found to be a critical parameter for controlling the crystalline structure.

Two alternative routes were used for the drying of the solids: spray drying and boiling under continuous stirring. It was found out that the two different drying procedures resulted in powders with very different shape, although it had no significant influence on the final surface area and porosity of the solids. In fact, no large differences in the capture properties of the two samples were observed.

Li_2ZrO_3 prepared by the soft-chemistry route calcined at 873 K could hold CO_2 in amounts equivalent to 27 wt%, and saturation was reached in less than 5 min at 848 K and 100% of CO_2. These results represent important improvements in the carbon dioxide capture rates compared to monoclinic Li_2ZrO_3 prepared by solid-state reactions with larger crystallite size. Figure 4.1 shows a direct comparison of the experimental data obtained in this work with data previously reported. Pure Li_2ZrO_3 prepared in this work is much faster than pure [74, 78] and K-doped [73] Li_2ZrO_3 prepared by solid-state reaction. Similar observations have also recently been reported by Yi *et al.* [83]. It should be noticed that the testing conditions of the compared samples are slightly different from the conditions used in this work.

An operating window for CO_2 capture was found at temperatures between 773 and 873 K, whereas the maximum rate was obtained at 848 K. Higher temperatures resulted in slower kinetics due to the importance of the reverse reaction. On the other hand, the capture rate decreased by decreasing the relative CO_2 amount. Very slow capture rates are observed at partial pressures of CO_2 below 0.1 bar as illustrated in Figure 4.2. The limitations on capture at low partial pressures of CO_2 are due to thermodynamic and/or diffusion limitations. The regeneration time was also strongly dependent on the regeneration temperature. The nanocrystalline properties of Li_2ZrO_3 prepared in this study also allowed faster regenerations in inert atmospheres.

Finally, as-prepared Li_2ZrO_3 showed good stability in dry conditions during multi-cycle operation. It was shown that the total capacity of the acceptor was maintained above 90% of the capacity of the fresh sample after 100 cycles. However, the appearance and disappearance of an induction period during the CO_2 capture on Li_2ZrO_3 has been observed. The reason for this reversible phenomenon is not clear.

The soft-chemistry route described in this work is a simple procedure that allows the preparation of Li_2ZrO_3 in a single step. The tetragonal and nanocrystalline nature of the resulting Li_2ZrO_3 give rise to improved capture of CO_2 in a wide range of temperatures. In addition, kinetics of the regeneration have also been improved, allowing fast regeneration in inert atmospheres at relatively low temperatures.

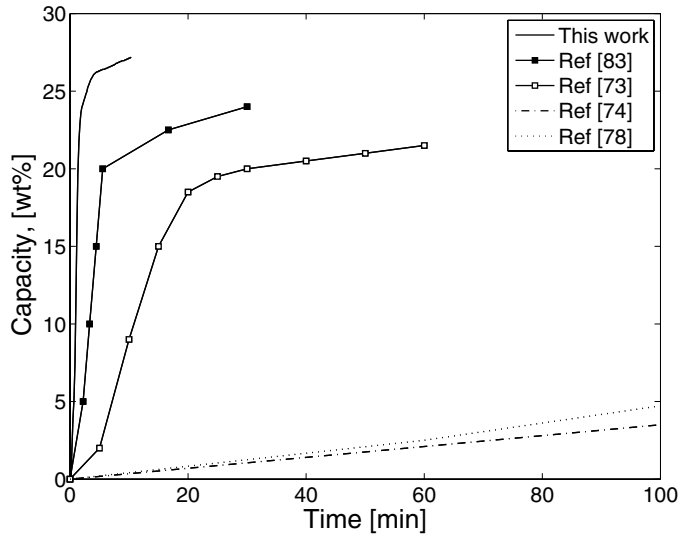

Figure 4.1: Comparison of the CO_2 capture properties of Li_2ZrO_3 prepared by the soft-chemistry route with other reported samples. $P_{CO_2} = 1$ bar. T=848 K (this work), 773 K (references [73, 83]), 873 K (references [74, 78]).

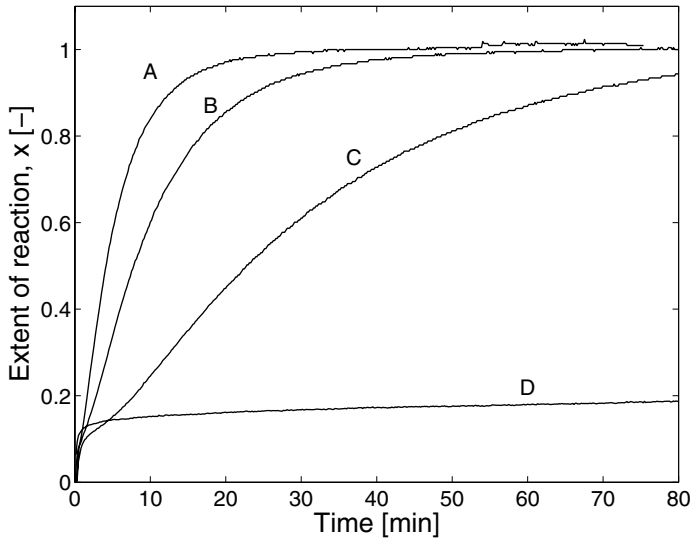

Figure 4.2: CO_2 uptake profiles using Li_2ZrO_3 as acceptor at 823 K and P_{CO_2} equal to (A) 0.7, (B) 0.5, (C) 0.3, and (D) 0.1 bar, respectively.

4.2 Paper III: Compositional effects on the CO_2 capture properties of Li_2ZrO_3

The soft-chemistry route where zirconyl nitrate and lithium acetate are used as precursors for preparation of nanocrystalline Li_2ZrO_3 has been further modified in order to study different compositional effects and optimise the working properties of Li_2ZrO_3. Special attention has been given to study the effect of different Li_2O-ZrO_2 stoichiometries on the CO_2 capture rates of pure lithium zirconate. In addition, the partial substitution of Li_2O with K_2O as a promoter has also been addressed. A detailed characterisation of all the prepared samples has been carried out and special attention has been given to understand the influence of the modifications on the composition of lithium zirconate on its properties as a CO_2 acceptor, such as CO_2 capture kinetics and stability.

It has been found that both the capture rate and capacity of lithium zirconate depend considerably on the Li_2O to ZrO_2 ratio, while the physical properties are very similar. Enhanced capture rates are observed when a deficiency of Li_2O is introduced ($Li_{1.8}ZrO_{2.9}$). Deficiency of Li_2O in the nominal composition results in relatively large amounts of excess ZrO_2. At these conditions, excess ZrO_2 is inert and will not take part in the reactions. It is suggested that excess ZrO_2 dispersed in between Li_2ZrO_3 will hinder crystal growth of Li_2ZrO_3 and enhance the grain boundary density of the material. Smaller crystallites and higher grain boundary density may enhance the reaction kinetics. Figure 4.3 shows the uptake profiles of three Li_2ZrO_3 samples with different stoichiometries. It is clear that the sample with Li deficiency shows consistently faster kinetics. In addition, the presence of secondary phases as ZrO_2 or Li_2CO_3 decrease the total theoretical capacity, but help for the total utilisation of the acceptors. In fact, larger extent of reaction is identified for the non-stoichiometric samples. The enhanced acceptor properties of non-stoichiometric two-phase materials are related to the heterogeneous phase boundaries introduced.

Moreover, the addition of K_2O results in improved capture rates due to the presence of molten carbonates. It is generally accepted that doping with potassium favours the diffusion of CO_2 through the Li_2CO_3 layer that is formed on the surface of the acceptor during the capture reaction. Due to the eutectic mixture between Li_2CO_3 and K_2CO_3, this layer will be totally or partially in a liquid phase at the reaction and regeneration conditions facilitating the diffusion of CO_2. Figure 4.4 shows the CO_2 uptake profiles of $K_{0.2}Li_{0.6}ZrO_{2.9}$ and $Li_{1.8}ZrO_{2.9}$ at four partial pressures of CO_2. It can be observed that the sub-

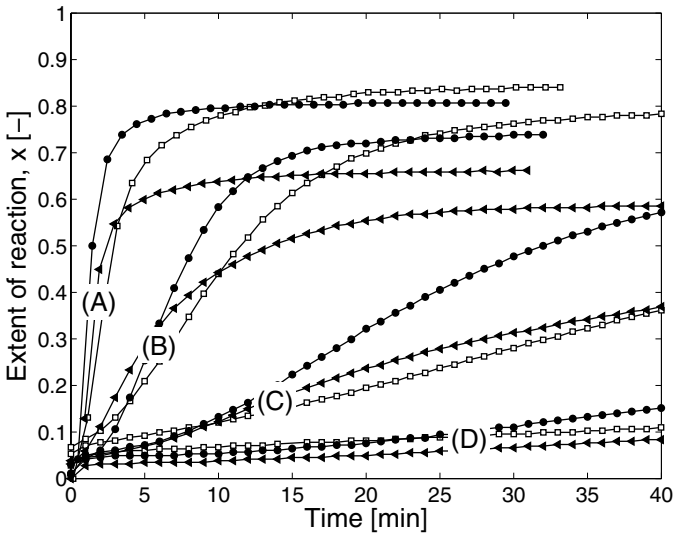

Figure 4.3: Uptake profiles at 848 K and (A): P_{CO_2}= 1 bar, (B): P_{CO_2}= 0.5 bar, (C): P_{CO_2}= 0.3 bar and (D): P_{CO_2}= 0.1 bar. (◄ = Li_2ZrO_3, □ = $Li_{2.2}ZrO_{3.1}$, • = $Li_{1.8}ZrO_{2.9}$)

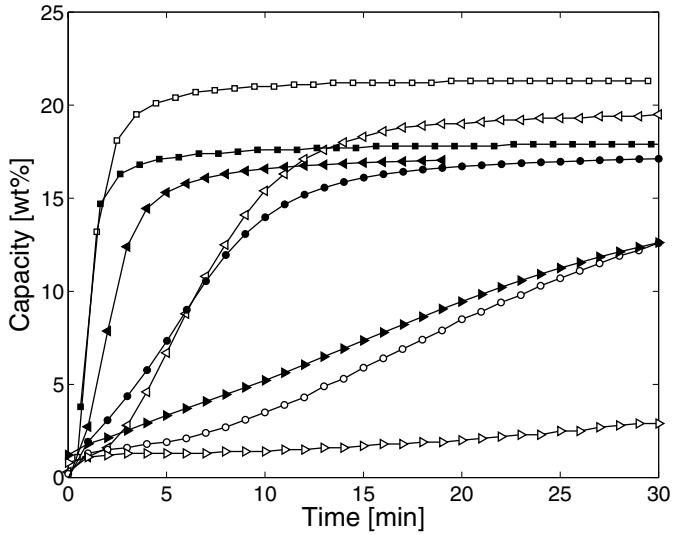

Figure 4.4: Uptake profiles at 848 K on $K_{0.2}Li_{0.6}ZrO_{2.9}$ (filled symbols) and $Li_{1.8}ZrO_{2.9}$ (open symbols), respectively. (■: P_{CO_2}= 1 bar, ◄: P_{CO_2}= 0.5 bar, •: P_{CO_2}= 0.3 bar, and ►: P_{CO_2}= 0.1 bar).

stitution of Li with K results in much faster kinetics, especially at low partial pressures of CO_2.

However, introduction of K_2O resulted in lower capacities and poorer stability probably due to particle coarsening. Adding larger amounts of K_2O resulted in improved kinetics, but also worse stability. Therefore, when doping with potassium, a compromise between kinetic enhancement and stability exists.

To summarise, controlling the Li_2O:ZrO_2 ratio is a very important parameter that can result in improved CO_2 uptake rates and better utilisation of the solid acceptor. The promotion with potassium is also beneficial in terms of kinetics, but a compromise between kinetic enhancement and stability should be considered. In addition, it has been shown that the soft-chemistry method earlier developed for fabrication of pure lithium zirconate has been modified with success for preparation of promoted samples with better kinetics than their counterparts prepared by solid-state reaction.

4.3 Paper IV: Synthesis and properties of Na_2ZrO_3 as a CO_2 acceptor

A novel method to produce nanosized Na_2ZrO_3 with a well-controlled crystal phase has been developed, resulting in excellent kinetics for CO_2 capture at high temperatures. The preparation method involves a soft-chemical route starting with the generation of a complex from zirconyl nitrate and sodium citrate. This is followed by a strong exothermal reaction between nitrate and citrate during calcination in a controlled atmosphere. A detailed preparation procedure is given in section 3.1.2.

It has been shown that the crystalline structure of Na_2ZrO_3 is strongly dependent on the calcination conditions. Relatively pure monoclinic Na_2ZrO_3 is produced by a two-step calcination procedure. First, the precursor was treated from room temperature to 1073 K at 10 K/min under argon flow, and then calcined at this temperature for 3 h under air. The *in situ* produced carbon during the first step of the calcination serves as a dispersant of the oxide. Subsequent carbon burn-off, during the second step, promotes the formation of nanocrystalline monoclinic Na_2ZrO_3 with open pore structures. The calcination temperature and atmosphere is crucial for controlling the crystal phase of Na_2ZrO_3; calcination at higher temperatures resulted mainly in hexagonal Na_2ZrO_3.

A kinetic study of CO_2 capture in a tapered element oscillating microbalance

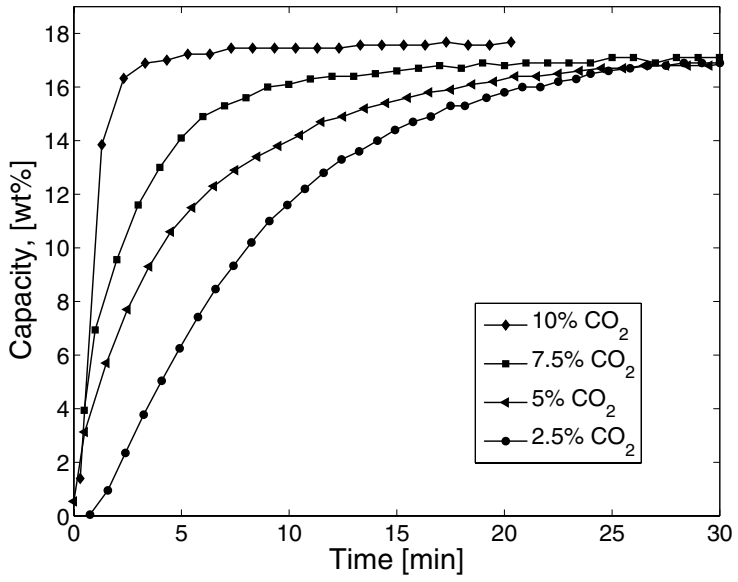

Figure 4.5: CO_2 uptake profiles on monoclinic Na_2ZrO_3 at 848 K and different CO_2 partial pressures.

(TEOM) reactor has shown that the monoclinic Na_2ZrO_3 is much more active than its hexagonal counterpart. This difference was attributed to the surface reactivity of the different crystalline phases. On the other hand, the ability to work at CO_2 partial pressures as low as 0.025 bar, together with the good stability in multi-cycle operation at dry conditions, makes nanocrystalline Na_2ZrO_3 a very promising CO_2 acceptor for different applications. Figure 4.5 shows the CO_2 uptake profiles of monoclinic Na_2ZrO_3 at different CO_2 partial pressures. These results represent a large improvement compared to the kinetics reported on similar materials [78]. Na_2ZrO_3 prepared by solid-state reactions has earlier been proposed as a good candidate for CO_2 removal using pure CO_2 as a probe gas. In that investigation 10 min were needed for saturation of the acceptor in 100% CO_2.

Summarising, a simple route for the formation of nanosized metal oxides with a well-defined crystal phase has been developed. This route may be a promising platform to synthesise oxide materials for selected applications.

4.4 Paper V: Effect of steam on the properties of ceramic CO_2 acceptors

The purpose of this study has been to systematically investigate the effect of water addition on the stability and CO_2 capture and regeneration properties of Li_2ZrO_3, K doped Li_2ZrO_3, Na_2ZrO_3 and Li_4SiO_4 at relevant SESMR conditions.

Typical steam contents in SESMR are higher than 30% and it is therefore important to investigate how the capture kinetics are affected at these environments. It has been shown that the addition of steam has a positive effect on the CO_2 uptake rate of all the studied acceptors. It is believed that the presence of steam enhances the Li^+, K^+ and Na^+ mobility, and therefore influences the rate of the reactions. Simultaneously, the diffusion of CO_2 through the carbonate layer formed during the carbonation reaction might also be favoured by steam. The formation of carbonates can enhance the diffusion rate. Similarly, the presence of steam also favours the regeneration kinetics. Figure 4.6 shows the positive effect of adding steam on the capture and regeneration kinetics of potassium promoted Li_2ZrO_3.

However, steam has a detrimental effect on the stability of the acceptors. Figure 4.7 shows the stability profiles of the acceptors included in this study in the presence and absence of steam. During dry operation, the capture was in all cases carried out at 848 K and 50% CO_2, while the regeneration was carried out in pure Ar at 923 K for Li_2ZrO_3 and K doped Li_2ZrO_3 and at 953 K for Na_2ZrO_3 and Li_4SiO_4. Under wet operation the capture was carried out at 848 K, 50% CO_2 and 20% H_2O, while the regeneration was carried out in a mixture of Ar and H_2O (8:2) at 923 K for Li_2ZrO_3 and K doped Li_2ZrO_3, at 953 K for Na_2ZrO_3, and at 848 K for Li_4SiO_4. Figure 4.7 evidences that all the acceptors show good stability in dry conditions. However, after reacting with steam during capture and regeneration, a large deactivation of the acceptors is observed, especially for the K doped sample. The decay in capacity could be ascribed both to phase segregation, sintering and vaporisation of alkali metals.

4.5 Paper VI: Catalysts for sorption-enhanced steam methane reforming

In this study, a series of hydrotalcite-based Ni catalysts with different loadings have been prepared by co-precipitation of $Mg(NO_3)_2 \cdot 6H_2O$, $Al(NO_3)_3 \cdot 9H_2O$ and $Ni(NO_3)_2 \cdot 6H_2O$ and compared with catalyst prepared by conventional incipient wetness impregnation. In particular, studying the effect of the

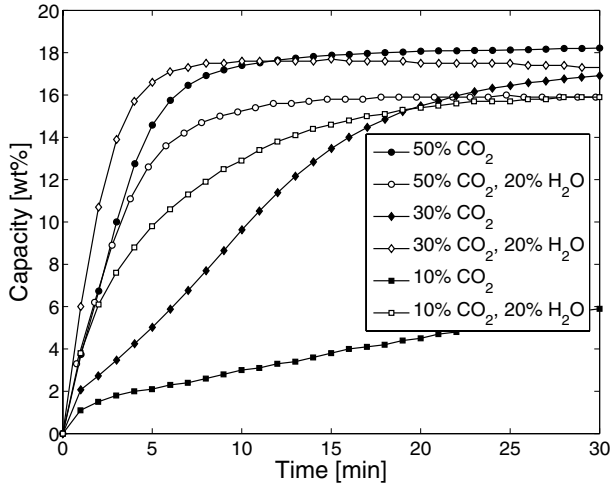

(a) Capture

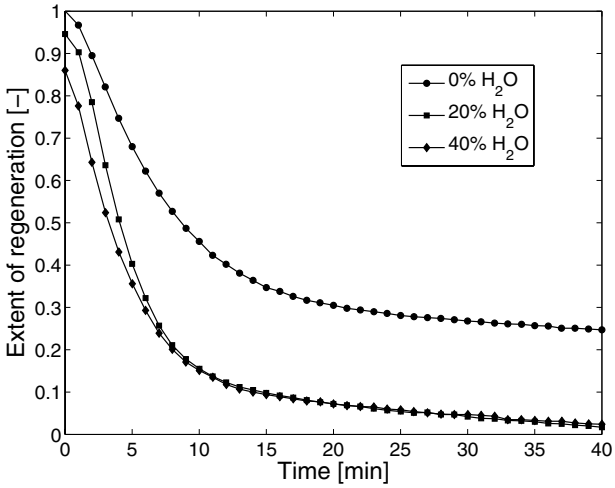

(b) Regeneration

Figure 4.6: Capture (848 K) and regeneration (923 K) profiles with and without steam addition for potassium promoted Li_2ZrO_3.

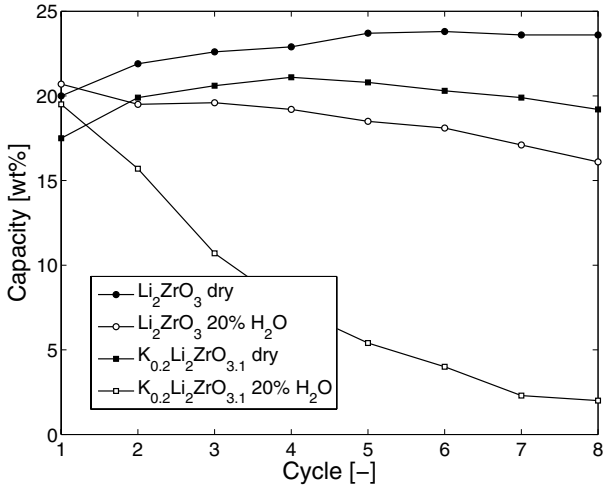

(a) Li_2ZrO_3 and K doped Li_2ZrO_3

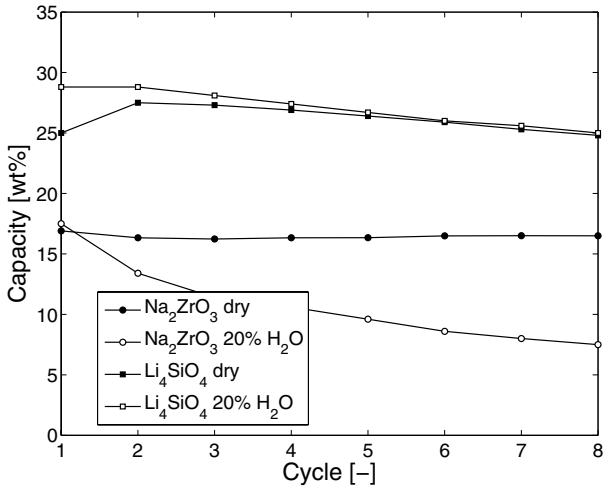

(b) Na_2ZrO_3 and Li_4SiO_4

Figure 4.7: Capacity stabilities of the acceptors in dry and wet conditions.

preparation method on the Ni distribution and on the stability and activity of the catalyst under steam reforming sintering conditions has been the main objective of the investigation.

Three different catalysts were prepared by the co-precipitation route: 12.5 Ni/HT, 40 Ni/HT and 77.5 Ni/HT. An additional sample (12.5 Ni/HT70) was prepared by incipient wetness impregnation of $Ni(NO_3)_2 \cdot 6H_2O$ on HT70, a commercial hydrotalcite support from Condea with $MgO/Al_2O_3 = 70/30$. Also a commercial SMR catalyst (CC) was used as a reference for comparison. The composition and main properties of the prepared catalysts are given in Table 4.1.

It can be observed that the co-precipitation technique results in more highly dispersed catalysts than incipient wetness impregnation, even at high loadings. A simple evaluation of the two preparation methods can be done by comparison of the catalysts 12.5 Ni/HT70 and 12.5 Ni/HT which have a similar composition, but were prepared by different routes. Both catalysts have comparable surface area, however, the dispersion of metallic Ni is higher on 12.5 Ni/HT, resulting in smaller crystals and higher Ni surface area. In addition, high Ni loading catalysts can be prepared by the co-precipitation technique. Dispersion and crystal size remained practically unchanged when the Ni loading was increased to 40 wt% (40 Ni/HT), while the Ni surface area increased considerably. However, the samples prepared by co-precipitation were more difficult to reduce. The different reduction behaviour can be explained by a stronger incorporation of Ni into the hydrotalcite for the catalysts prepared by co-precipitation. This gives smaller metallic particles as was observed from the H_2 chemisorption measurements.

Table 4.1: Catalysts composition and properties.

Catalyst	Ni loading [wt%]	BET surface area[a] [m^2/g_{cat}]	Ni surface area[b] [m^2 Ni/g_{cat}]	D^b [%]
12.5 Ni/HT	12.5	236	9.4	11.9
40 Ni/HT	40	153	28.0	10.8
77.5 Ni/HT	77.5	104	28.3	5.5
12.5 Ni/HT70	12.5	228	3.5	4.2
CC[c]	12.5	5.5	1.3	1.5

[a] Calculated from N_2 physisorption.
[b] Calculated from H_2 chemisorption. D: dispersion.
[c] Comercial catalyst.

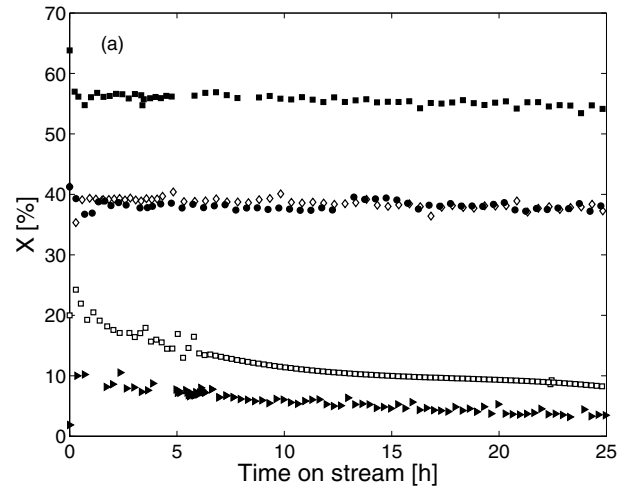

(a) Conversion

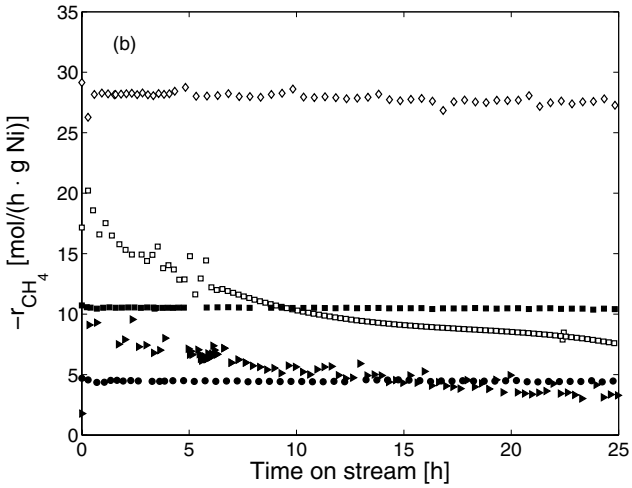

(b) Reaction rate per gram of Ni

Figure 4.8: Steam reforming of CH_4 at 923 K, S/C=3, 10 mg catalyst on (◇): 12.5 Ni/HT, (■): 40 Ni/HT, (●): 77.5 Ni/HT, (□): 12.5 Ni/HT70, and (►): CC.

The catalytic activity and stability of the prepared catalysts for the steam reforming of methane are shown in Figure 4.8. The results show that the Ni supported catalysts prepared by co-precipitation have highest activity and stability at the studied conditions. During the co-precipitation method, Ni is more homogeneously distributed in the bulk of the mixed oxides. During calcination, a large amount of the Ni migrates to the surface to form the highly dispersed and stable metal particles [50]. Although 12.5 Ni/HT showed most favourable kinetics, 40 Ni/HT might be the best candidate for application in SESMR since it displayed highest conversion per gram of catalyst. The use of 40 Ni/HT as catalyst will minimise the reactor volume which is a critical parameter in the process design.

It can be concluded that hydrotalcite-derived oxide mixtures are good supports providing efficient anchoring sites for Ni nanoparticles. Co-precipitation results in a stronger interaction between the support and nickel than incipient wetness. This results in smaller Ni crystals with good stability and high activity in steam reforming of methane. In addition, dispersion and crystal size were independent of Ni loading when increased from 12.5 to 40 wt% (40 Ni/HT) indicating that the direct synthesis of Ni based hydrotalcite is a promising way for preparing nanocrystals.

4.6 Paper VII: Sorption-enhanced steam reforming using Li_2ZrO_3 and Na_2ZrO_3 as CO_2 acceptors

Sorption-enhanced steam methane reforming has been carried out by using both Li_2ZrO_3 and Na_2ZrO_3 as acceptors. The reaction was performed in a stainless-steel fixed-bed reactor with inner diameter of approximately 16 mm. The reforming reactions were carried out at 848 K, 5 bar, steam-to-carbon ratio 5, acceptor-to-catalyst ratio 5 and total flow of 47 ml/min CH_4. Figure 4.9 shows a typical effluent concentration profile on a water free basis when Na_2ZrO_3 is used as acceptor. A H_2 yield above 97% is obtained for a period of time of 20 min. The main impurity was unconverted methane. The downstream composition remained unchanged until the saturation of the acceptor. At this point, breakthrough of the CO_2 took place and the conversion of methane decreased following the thermodynamics of conventional steam methane reforming. Accordingly, the H_2 yield decreased to approximately 69%.

The same experiment was carried out using Li_2ZrO_3 as acceptor. However, the H_2 yield was not considerably enhanced in this case due to kinetic limitations during the CO_2 removal. The capture reaction cannot compete with the re-

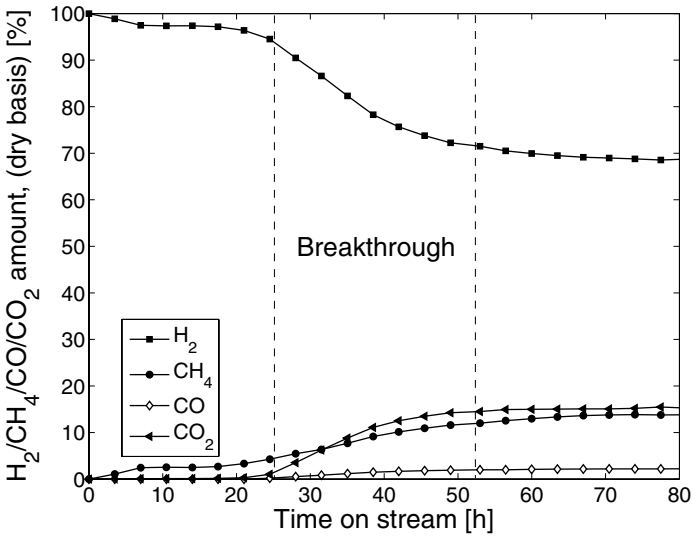

Figure 4.9: Effluent concentration profiles on a water free basis. 7.25 g Na_2ZrO_3, 1.45 g Ni catalyst, 848 K, S/C:5, 5 bar, 47 ml/min CH_4. Regeneration: 1023 K in Ar.

forming and the CO_2 formed in the reaction zone is not completely removed. Therefore, the obtained H_2 was very close to the thermodynamic equilibrium of conventional SMR at these conditions (67.9% H_2). Fixed-bed reactor simulations using a dynamic one-dimensional pseudo-homogeneous model have shown that higher H_2 yields can be obtained by using Li_2ZrO_3 as acceptor, but much lower space velocities than used in this work are required [86].

After saturation of the acceptors, the samples were regenerated in Ar at 1023 K. Later, the cycle was repeated several times to check the stability of the process. The conversion of methane and, as a consequence, the H_2 yield decreased dramatically during the second cycle. Presumably, the catalyst was poisoned by impurities from the CO_2 acceptor. Although the conversion decreased, the CO and CO_2 levels were below 0.5%. This happened when using both Li_2ZrO_3 and Na_2ZrO_3. The reason for this contamination is still not clear. However, it has been shown that the impurities could be partially removed after one operation cycle, most likely removed with steam.

Summarising, Li_2ZrO_3 and Na_2ZrO_3 have been tested as CO_2 acceptors for SESMR. H_2 yields higher than 95% in a single step were obtained by using Na_2ZrO_3 as acceptor. No such enhancement in the H_2 yield was observed when

Li_2ZrO_3 was used due to low CO_2 capture kinetics at low partial pressures of CO_2. Interaction between the catalyst and the acceptor has been observed, resulting in catalyst deactivation. The acceptor could be recovered and operated for several cycles, but still some deactivation was observed. Further studies are necessary in order to understand and control the deactivation processes that are hampering the application of these materials in sorption-enhanced steam methane reforming.

4.7 Paper VIII: Process design simulation of sorption-enhanced steam methane reforming

A large number of experimental and reactor modelling studies on SESMR have been reported, especially by application of CaO and hydrotalcite-like acceptors. However, little attention has been given to optimise the system configuration and the properties of the acceptor. In the present study, hydrogen production with CO_2 capture by SESMR is evaluated according to a multiscale approach. First, a process configuration has been proposed, simulated and discussed in terms of energy efficiency. Conventional steam methane reforming has been used as a base case for comparison. In addition, an evaluation of CaO, Li_2ZrO_3, K-doped Li_2ZrO_3, Na_2ZrO_3 and Li_4SiO_4 as potential CO_2 acceptors for SESMR has been carried out. The different candidates have been screened by means of thermodynamic analysis, kinetic measurements and process design simulations.

According to the thermodynamic analysis of the system, the hydrogen yield obtained by SESMR highly much dependent on the CO_2 acceptor properties. An acceptor working efficiently at low partial pressures of CO_2 is required. Figure 4.10 shows the equilibrium partial pressures for the acceptors selected in this study in the temperature interval from 725 to 1000 K. CaO shows more favourable equilibrium than the Li and Na based mixed oxides. For instance, a H_2 yield close to 90% can be achieved when the process is operated at 848 K, total pressure of 10 bar and Li_2ZrO_3 or Na_2ZrO_3 as acceptors, while a yield higher than 98% can be achieved with CaO at the same working conditions. Only 82% will be obtained by using Li_4SiO_4.

The thermal efficiencies of SESMR derived from the process simulation study also strongly depend on the CO_2 acceptor used. The SESMR case was modelled as a thermal/pressure swing process where the reformer operated at 10 bar and the regenerator at 1 bar. The reformer was modelled as a reactor with continuous regeneration of the acceptor. Both processes, SMR and SESMR,

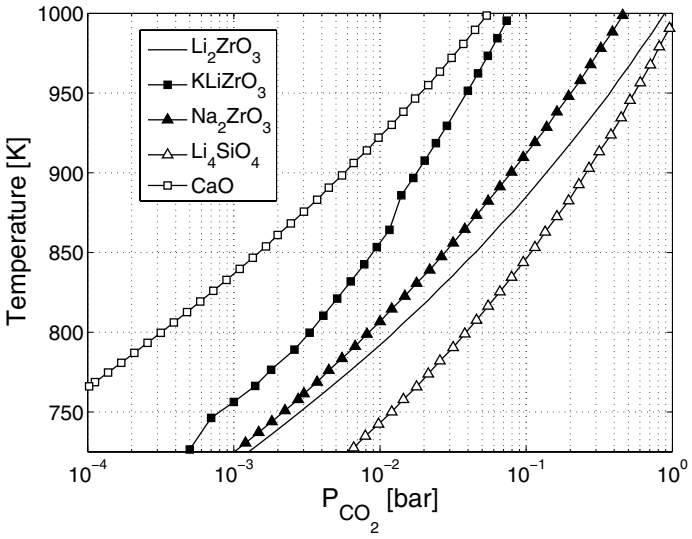

Figure 4.10: Equilibrium partial pressures of carbon dioxide for the different studied acceptors.

were simulated to obtain 99.9% H_2 at 25 bar and high purity CO_2 at 1 bar. For details about the process configuration and simulation conditions, the reader is referred to the full-text version of Paper VIII. The results show that similar efficiencies are obtained in SESMR when Li_2ZrO_3 is used as acceptor, as in conventional steam reforming followed by a CO_2 absorption unit. The use of an acceptor with a more favourable CO_2 equilibrium such as CaO considerably enhances this efficiency (about 82%). At the same time, SESMR gives a simpler process configuration, less demand of high temperature materials and smaller PSA units.

In addition to favourable thermodynamics, appropriate CO_2 capture kinetics and stability are also important properties for the application of CO_2 acceptors in SESMR. Large differences in the uptake kinetics of the different acceptors have been observed. In fact, CaO and Na_2ZrO_3 show considerably higher rates than Li_4SiO_4 and pure/promoted Li_2ZrO_3, both at high and low partial pressures of CO_2. Pure Li_2ZrO_3 showed the poorest performance. In terms of stability on dry atmospheres, the ceramic acceptors showed a good performance. However, CaO suffered a large decay in capacity after several cycles.

Therefore, combining the thermodynamic, stability and kinetic results, it can be concluded that none of the acceptors completely fulfil all the requirements for SESMR. CaO is the most favourable acceptor from the thermodynamic point of view leading to the highest H_2 yields. However, further development of the material is necessary in order to improve its stability. Na_2ZrO_3 may be a good alternative due to the good kinetics and stability in dry conditions, but an increase in the total capacity is desirable. It should be noticed that recent results show that the stability of Na_2ZrO_3 can be significantly lowered when operating at high pressures of steam (Paper V).

Summarising, the application of SESMR has been evaluated according to a multiscale approach and compared to conventional SMR. According to the thermodynamic analysis of the system, the hydrogen yield obtained by SESMR and efficiency are very much dependent on the CO_2 acceptor properties. It has been shown that sustainable production of pure H_2 with CO_2 capture with reasonable efficiencies is possible. However, a detailed economic evaluation of the system is necessary.

Chapter 5

Concluding remarks

The development of novel high-temperature CO_2 acceptors for application in sorption-enhanced steam methane reforming has been the scientific objective of this work. It has been shown that the properties of the CO_2 acceptor such as capacity, carbonation/calcination kinetics, regeneration temperature and stability have a direct impact on the feasibility of SESMR. The CO_2 acceptor will define the maximum H_2 yield, productivity and total efficiency of the process. Therefore, the design of an optimum CO_2 acceptor is not a trivial task. A good understanding of the relationship between chemical and physical properties of the materials and their activity for CO_2 capture is essential for the development of CO_2 acceptors.

The use of Li_2ZrO_3, potassium promoted Li_2ZrO_3, Li_4SiO_4, and Na_2ZrO_3 as CO_2 acceptors has been addressed in this work. It has been shown for Li_2ZrO_3 and Na_2ZrO_3 that controlling the crystalline phase and crystal size is crucial in order to optimise the CO_2 capture properties of the materials. The soft-chemistry route used in this study results in nanosized oxides with improved capture and regeneration properties. In terms of capture kinetics, Na_2ZrO_3 has been shown to be superior compared to the other acceptors. However, Na_2ZrO_3 suffers from low capacity and requires higher temperatures for regeneration. It should also be mentioned that the different ability for CO_2 removal observed for the various acceptors could not be ascribed to the textural properties of the oxides. In fact, a better understanding of the reaction mechanisms of carbonation and calcination is necessary in order to clarify this issue and to be able to design acceptors with improved properties.

The more favourable kinetics of Na_2ZrO_3 for removing CO_2 make it more suitable for application in SESMR than the other ceramic acceptors, allowing the production of hydrogen yields above 95% with a higher throughput. However, there are still several limitations concerning the use of ceramic acceptors in SESMR. Firstly, a pronounced decay in the capacity is observed when operating under large partial pressures of steam. In addition, it has been observed that the acceptors interact with the catalyst, resulting in catalyst deactivation, most likely due to the alkaline metals blocking the Ni sites. However, no such deactivation was observed when using the commercial Li_4SiO_4 sample. Therefore, it is believed that the poisoning might be due to impurities present in the in-house prepared acceptors. This is a matter that should be further investigated. Attention should also be given to the attrition properties of such materials, especially if a fluidised-bed reactor is chosen as the preferred configuration.

Furthermore, it is necessary to study the long term multi-cycle properties of ceramic acceptors under steam during many more cycles than in this work. Ceramic acceptors must be able to withstand many cycles in order to compete with inexpensive natural sorbents such as dolomite. An economic evaluation of SESMR is necessary at this point which will clarify the target with respect to the durability of the acceptors.

Summarising, it has been demonstrated that SESMR is a promising route for production of high purity H_2 with CO_2 management. Ceramic acceptors might be chosen as CO_2 acceptors, but still some work is needed to understand their reaction mechanism, improve their working properties, and specially optimise their integration with the catalyst. Further studies are necessary in order to understand and control the catalyst deactivation observed during SESMR operation with ceramic acceptors. This problem can make the application of Li_2ZrO_3 and Na_2ZrO_3 in SESMR difficult.

Alternatively, synthetic Ca-based acceptors could be used. These sorbents have recently received increased attention due to their good stability.

Bibliography

[1] J.T. Houghton, Y. Ding, D.J. Griggs, M. Noguer, P.J. van der Linden, X. Dai, K. Maskell, and C.A. Johnson. *IPCC 2001: Climate Change 2001: The Scientific Basis.* Cambridge University Press, 2005.

[2] International Energy Agency. *Prospects for carbon dioxide capture and storage. Technical report, OECD/IEA.* 2003.

[3] G. Marland, T.A. Boden, and R.J. Andres. *Global, Regional, and National CO_2 Emissions. In Trends: A Compendium of Data on Global Change.* Oak Ridge National Laboratory, U.S. Department of Energy, Oak Ridge, USA, 2006.

[4] B. Metz, O. Davidson, H. de Coninck, M. Loos, and L. Meyer. *IPCC 2005: Special report on carbon dioxide capture and storage.* Cambridge University Press, 2005.

[5] O. Bolland. *Capture Technologies- an Overview. In The Second Trondheim Conference on CO_2 Capture, Transport and Storage.* 2004.

[6] S.S. Penner. Steps towards the hydrogen economy. *Energy*, 31:33–43, 2006.

[7] P. Zegers. Fuel cell commercialization: The key to a hydrogen economy. *J. Power Sources*, 154:497–502, 2006.

[8] T. Rostrup-Nielsen. Manufacture of hydrogen. *Catal. Today*, 106:293–296, 2005.

[9] J.N. Armor. Catalysis and the hydrogen economy. *Catal. Lett.*, 101:131–135, 2005.

[10] R. Bredesen, K. Jordal, and O. Bolland. High-temperature membranes in power generation with CO_2 capture. *Chem. Eng. Process.*, 43:1129–1158, 2004.

[11] B. Balasubramanian, A.L. Ortiz, S. Kaytakoglu, and D.P. Harrison. Hydrogen from methane in a single-step process. *Chem. Eng. Sci.*, 54:3543–3552, 1999.

[12] K. Nakagawa and T. Ohashi. A novel method of CO_2 capture from high temperature gases. *J. Electrochem. Soc.*, 145:1344–1346, 1998.

[13] J.R. Rostrup-Nielsen and T. Rostrup-Nielsen. Large-scale hydrogen production. *Catal. Technol.*, 6:150–159, 2002.

[14] FactSage 5. *The integrated thermodynamic databank system. www.factsage.com.*

[15] J.R. Hufton, S. Mayorga, and S. Sircar. Sorption-enhanced reaction process for hydrogen production. *AIChE J.*, 45:248–256, 1999.

[16] D.P. Harrison and Z. Peng. Low-carbon monoxide hydrogen production by sorption-enhanced reaction. *Int. J. Chem. Reactor Eng.*, 1:Article A37, 2003.

[17] K.B. Yi and D.P. Harrison. Low-pressure sorption-enhanced hydrogen production. *Ind. Eng. Chem. Res.*, 44:1665–1669, 2005.

[18] J.R. Rostrup-Nielsen. *Catalytic Steam Reforming. In Catalysis: Science and Technology.* Springer, 1984.

[19] R. Williams. *Hydrogen production, U.S. Patent 1,938,202.* 1933.

[20] E. Gorin and W.B. Retallick. *Method for the production of hydrogen, U.S. Patent 3,108,857.* 1963.

[21] C. Han and D.P. Harrison. Simultaneous shift reaction and carbon dioxide separation for the direct production of hydrogen. *Chem. Eng. Sci.*, 49:5875–5883, 1994.

[22] A. Siliban M. Narcida and D.P. Harrison. Characteristics of the reversible reaction between CO_2(g) and calcined dolomite. *Chem. Eng. Commun.*, 146:149–162, 1996.

[23] A. Lopez-Ortiz and D.P. Harrison. Hydrogen production using sorption-enhanced reaction. *Ind. Eng. Chem. Res.*, 40:5102–5109, 2001.

[24] N. Hildenbrand, J. Readman, I.M. Dahl, and R. Blom. Sorbent enhanced steam reforming (SESR) of methane using dolomite as internal carbon dioxide absorbent: Limitations due to $Ca(OH)_2$ formation. *Appl. Catal., A*, 303:131–137, 2006.

[25] K. Johnsen, H.J. Ryu, J.R. Grace, and C.J. Lim. Sorption-enhanced steam reforming of methane in a fluidised bed reactor with dolomite as CO_2-acceptor. *Chem. Eng. Sci.*, 61:1195–1202, 2006.

[26] K. Johnsen. Sorption-enhanced steam methane reforming in fluidised bed reactors. PhD thesis, Norwegian University of Science and Technology, Trondheim, Norway. 2006.

[27] K. Johnsen, J.R. Grace, S.S.E.H. Elnashaie, L. Kolbeinsen, and D. Eriksen. Modeling of sorption-enhanced steam reforming in a dual fluidised bubbling bed reactor. *Ind. Eng. Chem. Res.*, 45:4133–4144, 2006.

[28] Z. Li, N. Cai, and J. Yang. Continuous production of hydrogen from sorption-enhanced steam methane reforming in two parallel fixed-bed reactors operated in a cyclic manner. *Ind. Eng. Chem. Res.*, 45:8788–8793, 2006.

[29] V. Dupont, A.B. Ross, I. Hanley, and M.V. Twigg. Unmixed steam reforming of methane and sunflower oil: A single-reactor process for H_2-rich gas. *Int. J. Hydrogen Energy*, 32:67–79, 2007.

[30] R.K. Lyon and J.A. Cole. Unmixed combustion: An alternative to fire. *Combust. Flame*, 121:249–261, 2000.

[31] B.T. Carvill, J.R. Hufton, M. Anand, and S. Sircar. Sorption-enhanced reaction process. *AIChE J.*, 42:2765–2772, 1996.

[32] S. Sircar and M.B. Rao. Liquid-phase sorption-enhanced reaction process. *AIChE J.*, 42:2765–2772, 1999.

[33] W.E. Waldron, J.R. Hufton, and S. Sircar. Production of hydrogen by cyclic sorption enhanced reaction process. *AIChE J.*, 47:1477–1479, 2001.

[34] Y. Ding and E. Alpay. Adsorption-enhanced steam-methane reforming. *Chem. Eng. Sci.*, 55:3929–3940, 2000.

[35] G. Xiu, J.L. Soares, P. Li, and A.E. Rodrigues. Simulation of five-step one-bed sorption-enhanced reaction process. *AIChE J.*, 48:2817–2832, 2002.

[36] G. Xiu, P. Li, and A.E. Rodrigues. Sorption-enhanced reaction process with reactive regeneration. *Chem. Eng. Sci.*, 57:3893–3908, 2002.

[37] G. Xiu, P. Li, and A.E. Rodrigues. New generalized strategy for improving sorption-enhanced reaction process. *Chem. Eng. Sci.*, 58:3425–3437, 2003.

[38] G.H. Xiu, P. Li, and A.E. Rodrigues. Subsection-controlling strategy for improving sorption-enhanced reaction process. *Chem. Eng. Res. Des.*, 82:192–202, 2004.

[39] Y. Wang and A.E. Rodrigues. Hydrogen production from steam methane reforming coupled with in situ CO_2 capture: Conceptual parametric study. *Fuel*, 84:1778–1789, 2005.

[40] H.T.J. Reijers, S.E.A. Valster-Schiermeier, P.D. Cobden, and R.W. van den Brink. Hydrotalcite as CO_2 Sorbent for Sorption-Enhanced Steam Reforming of Methane. *Ind. Eng. Chem. Res.*, 45:2522–2530, 2006.

[41] S. Lin, M. Harada, Y. Suzuki, and H. Hatano. Hydrogen production from coal by separating carbon dioxide during gasification. *Fuel*, 81:2079–2085, 2002.

[42] A.A. Iordanidis, P.N. Kechagiopoulos, S.S. Voutetakis, A.A. Lemonidou, and I.A. Vasalos. Autothermal sorption-enhanced steam reforming of bio-oil/biogas mixture and energy generation by fuel cells: Concept analysis and process simulation. *Int. J. Hydrogen Energy*, 31:1058–1065, 2006.

[43] J.R. Rostrup-Nielsen. Production of synthesis gas. *Catal. Today*, 18:305–324, 1993.

[44] J. Wei and E. Iglesia. Isotopic and kinetic assessment of the mechanism of reaction of CH_4 with CO_2 or H_2O to form synthesis gas and carbon on nickel catalysts. *J. Catal.*, 224:370–383, 2004.

[45] H.S. Bengaard, J.K. Nørskov, J. Sehested, B.S. Clausen, L.P. Nielsen, A.M. Molenbroek, and J.R. Rostrup-Nielsen. Steam reforming and graphite formation on Ni catalysts. *J. Catal.*, 209:365–384, 2002.

[46] F. Trifirò, A. Vaccari, J. Sehested, and O. Clause. Nature and properties of nickel-containing mixed oxides obtained from hydrotalcite-type anionic clays. *Catal. Today*, 21:185–195, 1994.

[47] O. Clause, M. Goncalves Coelho, M. Gazzano, D. Matteuzzi, F. Trifirò, and A. Vaccari. Synthesis and thermal reactivity of nickel-containing anionic clays. *Appl. Clay Sci.*, 8:169–186, 1993.

[48] F. Cavani, F. Trifirò, and A. Vaccari. Hydrotalcite-type anionic clays: Preparation, properties and applications. *Catal. Today*, 11:173–301, 1991.

[49] G. Fornasari, M. Gazzano, D. Matteuzzi, F. Trifirò, and A. Vaccari. Structure and reactivity of high-surface-area Ni/Mg/Al mixed oxides. *Appl. Clay Sci.*, 10:69–82, 1995.

[50] K. Takehira, T. Shishido, P. Wang, T. Kosaka, and K. Takaki. Steam reforming of CH_4 over supported Ni catalysts prepared from a Mg-Al hydrotalcite-like anionic clay. *Phys. Chem. Chem. Phys.*, 5:3801–3810, 2003.

[51] Z. Yong, V. Mata, and A.E. Rodrigues. Adsorption of carbon dioxide at high temperature- A review. *Sep. Purif. Technol.*, 26:195–205, 2002.

[52] Z. Yong, V.G. Mata, and A.E. Rodrigues. Adsorption of CO_2 on chemically modified high surface area carbon-based adsorbents at high temperature. *Adsorption*, 7:41–40, 2001.

[53] M.M. Lila and J.F. Finn. Carbon dioxide adsorption on 5A zeolite designed for CO_2 removal in spacecraft cabins, NASA/TM-1998-208752. 1998.

[54] Y. Ding and E. Alpay. Equilibria and kinetics of CO_2 adsorption on hydrotalcite adsorbent. *Chem. Eng. Sci.*, 55:3461–3474, 2000.

[55] Z. Yong, V. Mata, and A.E. Rodrigues. Adsorption of carbon dioxide onto hydrotalcite-like compounds at high temperatures. *Ind. Eng. Chem. Res.*, 40:204–209, 2001.

[56] Z. Yong and A.E. Rodrigues. Hydrotalcite-like compounds as adsorbents for carbon dioxide. *Energy Convers. Manage.*, 43:1865–1876, 2002.

[57] N.D. Hutson. Structural effects on the high temperature adsorption on CO_2 on a synthetic hydrotalcite. *Chem. Mater.*, 16:4135–4143, 2004.

[58] B. Ficicilar and T. Dogu. Breakthrough analysis for CO_2 removal by activated hydrotalcite and soda ash. *Catal. Today*, 115:274–278, 2006.

[59] S.P. Reynolds, A.D. Ebner, and D.A. Ritter. Carbon dioxide capture from flue gas by pressure swing adsorption at high temperature using a K-promoted HTlc: Effects of mass transfer on the process performance. *Environ. Prog.*, 25:334–342, 2006.

[60] K.B. Lee, A. Verdooren, H.S. Caram, and S. Sircar. Chemisorption of carbon dioxide on potassium-carbonate-promoted hydrotalcite. *J. Colloid Interface Sci.*, 308:30–39, 2007.

[61] A.D. Ebner, S.P. Reynolds, and J.A. Ritter. Nonequilibrium kinetic model that describes the reversible adsorption and desorption behavior of CO_2 in a K-promoted hydrotalcite-like compound. *Ind. Eng. Chem. Res.*, 46:1737–1744, 2007.

[62] S.K. Bhatia and D.D. Perlmutter. Effect of the product layer on the kinetics on the CO_2-lime reaction. *AIChE J.*, 29:79–86, 1983.

[63] J.C. Abanades. The maximum capture efficiency of CO_2 using carbonation/calcination cycle of $CaO/CaCO_3$. *Chem. Eng. J.*, 90:303–306, 2002.

[64] D. Alvarez and J.C. Abanades. Pore-size and shape effects on the recarbonation performance of calcium oxide submitted to repeated calcination/recarbonation cycles. *Energy Fuels*, 19:270–278, 2005.

[65] D. Alvarez and J.C. Abanades. Determination of the critical product layer thickness in the reaction of CaO with CO_2. *Ind. Eng. Chem. Res.*, 44:5608–5615, 2005.

[66] J.C. Abanades and D. Alvarez. Conversion limits in the reaction of CO_2 with lime. *Energy Fuels*, 17:308–315, 2003.

[67] G.S. Grasa and J.C. Abanades. CO_2 capture capacity of CaO in a long series of carbonation/calcination cycles. *Ind. Eng. Chem. Res.*, 45:8846–8851, 2006.

[68] Z. Li, N. Cai Y. Huang, and H. Han. Shynthesis, experimental studies, and analysis of a new calcium-based carbon dioxide absorbent. *Energy Fuels*, 19:1447–1452, 2005.

[69] Z. Li, N. Cai, and Y. Hunag. Effect of preparation temperature on cyclic CO_2 capture and multiple carbonation-calcination cycles for a new Ca-based CO_2 sorbent. *Ind. Eng. Chem. Res.*, 45:1911–1917, 2006.

[70] B. Feng, W. Liu, and H. An. Overcoming the problem of loss in capacity of calcium oxide in CO_2 capture. *Energy Fuels*, 20:2417–2420, 2006.

[71] T. Ohashi and K. Nakagawa. Effect of potassium carbonate additive on CO_2 absorption in lithium zirconate powder. *Mat. Res. Soc. Symp. Proceed.*, 547:249–254, 1999.

[72] M. Kato and K. Nakagawa. New series of lithium containing complex oxides, lithium silicates, for application as a high temperature CO_2 absorbent. *J. Ceram. Soc. Jpn.*, 109:911–914, 2001.

[73] R. Xiong, J. Ida, and Y.S. Lin. Kinetics of carbon dioxide sorption on potasium-doped lithium zirconate. *Chem. Eng. Sci.*, 58:4377–4385, 2003.

[74] J. Ida and Y.S. Lin. Mechanism of High-Temperature CO_2 Sorption on Lithium Zirconate. *Environ. Sci. Technol.*, 37:1999–2004, 2003.

[75] J. Ida, R. Xiong, and Y.S. Lin. Synthesis and CO_2 sorption properties of pure and modified lithium zirconate. *Sep. Purif. Technol.*, pages 41–51, 2004.

[76] K. Essaki, K. Nakagawa, M. Kato, and H. Uemoto. CO_2 absorption by lithium silicate at room temperature. *J. Chem. Eng. Jpn.*, 37:772–777, 2004.

[77] B.N. Nair, T. Yamaguchi, H. Kawamura, and S. Nakao. Processing of lithium zirconate for applications in carbon dioxide separation: structure and properties of the powders. *J. Am. Ceram. Soc.*, 87:68–74, 2004.

[78] A. López-Ortiz, N.G.P. Rivera, A.R. Rojas, and D.L. Gutierrez. Novel Carbon Dioxide Solid Acceptors Using Sodium Containing Oxides. *Sep. Sci. Technol.*, 39:3559–3572, 2004.

[79] D.J. Fauth, J.S. Hoffman, and H.W. Pennline. Dry regenerable sorbents for the separation and capture of CO_2 from large point sources. *J. Environ. Technol. Manage.*, 4:68–81, 2004.

[80] H. Pfeiffer and P. Bosc. Thermal stability and high-temperature carbon dioxide sorption on hexa-lithium zirconate. *Chem. Mater.*, 17:1704–1710, 2005.

[81] S. Kimura, M. Adachi, R. Noda, and M. Horio. Particle design and evaluation of dry CO_2 recovery sorbent with a liquid holding capability. *Chem. Eng. Sci.*, 60:4061–4071, 2005.

[82] D.J. Fauth, E.A. Frommell, J.S. Hoffman, R.P. Reasbeck, and H.W. Pennline. Eutectic salt promoted lithium zirconate: Novel high temperature sorbent for CO_2 capture. *Fuel Process. Technol.*, 86:1503–1521, 2005.

[83] K.B. Yi and D.Ø. Eriksen. Low temperature liquid state synthesis of lithium zirconate and its characteristics as a CO_2 sorbent. *Sep. Sci. Technol.*, 41:283–296, 2006.

[84] H. Pfeiffer, C. Vazquez, V.H. Lara, and P. Bosc. Thermal behavior and CO_2 absorption of $Li_{2-x}Na_xZrO_3$ solid solutions. *Chem. Mater.*, 19:922–926, 2007.

[85] M. Kato, S. Yoshikawa, and K. Nakagawa. Carbon dioxide absorption by lithium orthosilicate in a wide range of temperature and carbon dioxide concentrations. *J. Mater. Sci. Lett.*, 21:485–487, 2002.

[86] E. Ochoa-Fernández, H.K. Rusten, H.A. Jakobsen, M. Rønning, A. Holmen, and D. Chen. Sorption enhanced hydrogen production by steam methane reforming using Li_2ZrO_3 as sorbent: Sorption kinetics and reactor simulation. *Catal. Today*, 106:41–46, 2005.

[87] C. Alvani, L. Bruzzi, S. Casadio, V. Rondinella, A. Tucci, and E.H. Toscano. Preparation of lithium zirconate by powder reaction and hydrolysis of metal alcoxides. *J. Eur. Ceram. Soc.*, 5:295–302, 1989.

[88] J.Y. Park, C.H. Jung, S. Oh, H.K. Park, and Y.S. Kim. Preparation of lithium zirconate powders by the combustion process. *Ceram. Trans.*, 85:55–66, 1997.

[89] L. Montanaro and J.P. Lecompte. Preparation via gelling of porous lithium zirconate for fusion reactor blanket material. *J. Mater. Sci.*, 27:3763–3769, 1992.

[90] D. Vollath and H. Wedemeyer. Process for the preparation of lithium metazirconate. *J. Nucl. Mat.*, 179:793–795, 1991.

[91] J.C. Abanades, E.S. Rubin, and E.J. Anthony. Sorbent cost and performance in CO_2 capture systems. *Ind. Eng. Chem. Res.*, 43:3462–3466, 2004.

[92] Bruker AXS. DIFFRAC^{plus} EVA Release 2001 Version 7.0 rev.0. 2:98, 2001.

[93] P. Scherrer. Bestimmung der Grösse und der inneren Struktur von Kolloidteil mittels Röntgenstrahlen. *Göttingen Nachrichten*, 2:98–100, 1918.

[94] S. Brunauer, P.H. Emmett, and E. Teller. Adsorption of gases in multimolecular layers. *J. Am. Chem. Soc.*, 60:309–319, 1938.

[95] E.P. Barrett, L.G. Joyner, and P.P. Halenda. The determination of pore volume and area distributions in porous substances. I. Computations from nitrogen isotherms. *J. Am. Chem. Soc.*, 73:373–380, 1951.

[96] E.A. Blekkan, A. Holmen, and S. Vada. Alkali promotion of alumina-supported cobalt Fischer-Tropsch catalysts studied by TPR, TPD and pulse chemisorption. *Acta Chem. Scand.*, 47:275–280, 1993.

[97] D. Chen, H.P. Rebo, K. Moljord, and A. Holmen. Effect of coke deposition on transport and adsorption in zeolites studied by a new microbalance reactor. *Chem. Eng. Sci.*, 51:2687–2692, 1996.

[98] D. Chen, E. Bjørgum, K.O. Christensen, A. Holmen, and R. Lødeng. Characterization of Catalysts under Working Conditions with an Oscillating Microbalance Reactor. *Adv. Catal.*, 51:351–382, 2007.

Papers are not included due to copyright.